

This discussion paper is/has been under review for the journal Atmospheric Measurement Techniques (AMT). Please refer to the corresponding final paper in AMT if available.

# Comparison of SMILES ClO profiles with other satellite and balloon-based measurements

**H. Sagawa<sup>1</sup>, T. O. Sato<sup>2,1</sup>, P. Baron<sup>1</sup>, E. Dupuy<sup>1,\*</sup>, N. Livesey<sup>3</sup>, J. Urban<sup>4</sup>,  
T. von Clarmann<sup>5</sup>, A. de Lange<sup>6</sup>, G. Wetzel<sup>5</sup>, A. Kagawa<sup>1</sup>, D. Murtagh<sup>4</sup>, and  
Y. Kasai<sup>1,2</sup>**

<sup>1</sup>Applied Electromagnetic Research Institute, National Institute of Information and Communications Technology, Nukui-kita, Koganei, Tokyo 184-8795, Japan

<sup>2</sup>Tokyo Institute of Technology, Nagatsuta, Midori-ku, Yokohama, Kanagawa 226-8503, Japan

<sup>3</sup>Jet Propulsion Laboratory, California Institute of Technology, 4800 Oak Groove Drive, Pasadena, California 91109, USA

<sup>4</sup>Department of Earth and Space Sciences, Chalmers University of Technology, 41296 Gothenburg, Sweden

<sup>5</sup>Karlsruhe Institute of Technology, Institute for Meteorology and Climate Research, P.O. Box 3640, 76021 Karlsruhe, Germany

<sup>6</sup>SRON-Netherlands Institute for Space Research, Sorbonnelaan 2, 3584 CA, Utrecht, The Netherlands

\*now at: National Institute for Environmental Studies, Onogawa, Tsukuba, Ibaraki 305-8506, Japan

Title Page

Abstract

Introduction

Conclusions

References

Tables

Figures

◀

▶

◀

▶

Back

Close

Full Screen / Esc

Printer-friendly Version

Interactive Discussion



Received: 18 December 2012 – Accepted: 24 December 2012 – Published: 17 January 2013

Correspondence to: H. Sagawa (sagawa@nict.go.jp)

Published by Copernicus Publications on behalf of the European Geosciences Union.

**AMTD**

6, 613–663, 2013

---

**SMILES CIO  
comparison**

H. Sagawa et al.

---

Title Page

Abstract

Introduction

Conclusions

References

Tables

Figures



Back

Close

Full Screen / Esc

Printer-friendly Version

Interactive Discussion



## Abstract

We evaluate the quality of ClO profiles derived from the Superconducting Submillimeter-Wave Limb-Emission Sounder (SMILES) on the International Space Station (ISS). Version 2.1.5 of the level-2 product generated by the National Institute of Information and Communications Technology (NICT) is the subject of this study. Based on error analysis simulations the systematic error was estimated as 5–10 pptv at the pressure range of 80–20 hPa, 35 pptv at the ClO peak altitude ( $\sim 4$  hPa), and 5–10 pptv at pressures  $\leq 0.5$  hPa for daytime mid-latitude conditions. For nighttime measurements, a systematic error of 8 pptv was estimated for the ClO peak altitude ( $\sim 2$  hPa). The SMILES NICT v2.1.5 ClO profiles agree with those derived from another level-2 processor developed by JAXA within of the bias uncertainties, except for the nighttime measurements in the low and middle latitude region where the SMILES NICT v2.1.5 profiles have a negative bias of  $\sim 30$  pptv in the lower stratosphere. This bias is considered to be due to the use of a limited spectral bandwidth in the retrieval process, which makes it difficult to distinguish between the ClO signal and wing contributions of spectral features outside the bandwidth. In the middle and upper stratosphere outside the polar regions, no significant systematic bias was found for the SMILES NICT ClO profile with respect to datasets from other instruments such as the Aura Microwave Limb Sounder (MLS), the Odin Sub-Millimetre Radiometer (SMR), and the Envisat Michelson Interferometer for Passive Atmospheric Sounding (MIPAS), which demonstrates the scientific usability of the SMILES ClO data including the diurnal variations. Inside the chlorine-activated polar vortex the SMILES NICT v2.1.5 ClO profiles show larger volume mixing ratios by 0.3 ppbv (30%) at 50 hPa compared to those of the JAXA processed profiles. This discrepancy is also considered to be an effect of the limited spectral bandwidth in the retrieval processing. We also compared the SMILES NICT ClO profiles of chlorine-activated polar vortex conditions with those measured by the balloon-borne instruments Terahertz and submillimeter Limb Sounder (TELIS) and the MIPAS-balloon (MIPAS-B).

## SMILES ClO comparison

H. Sagawa et al.

Title Page

Abstract

Introduction

Conclusions

References

Tables

Figures

◀

▶

◀

▶

Back

Close

Full Screen / Esc

Printer-friendly Version

Interactive Discussion



## 1 Introduction

It is well known that chlorine monoxide (ClO) is one of the key species for the ozone depletion mechanism in the stratosphere, participating to the reaction cycle as the primary element of the reactive chlorine family. It has therefore been a major target of scientific interest for several satellite and balloon-borne missions, for example, the UARS Microwave Limb Sounder (MLS) (Reber et al., 1993; Waters et al., 1993) and its successor Aura MLS (Waters et al., 2006), the Odin Sub-Millimetre Radiometer (SMR) (Murtagh et al., 2002), the Michelson Interferometer for Passive Atmospheric Sounding (MIPAS) (Fischer et al., 2008; Friedl-Vallon et al., 2004) onboard the Envisat satellite and the MIPAS-B2 gondola which supports also the Terahertz and submillimeter Limb Sounder (TELIS) (Birk et al., 2010).

The Superconducting Submillimeter-Wave Limb-Emission Sounder (SMILES) attached to the Japanese Experiment Module (JEM) on the International Space Station (ISS) performed ClO measurements with a sensitivity of an order of magnitude higher than other satellite-borne instruments due to its 4 K cooled superconducting receiver system (Kikuchi et al., 2010). Although its scientific findings are outside the scope of this paper, the SMILES ClO measurements provided several interesting insights into the stratospheric and mesospheric researches such as the global distribution of ClO in the middle atmosphere and its diurnal variations. In particular, these measurements observationally revealed the mesospheric diurnal variation of ClO for the first time (Sato et al., 2012).

The National Institute of Information and Communications Technology (NICT) in Japan has developed a retrieval processing chain for the SMILES data analysis. Sato et al. (2012) carried out a simulation study to assess the errors in the NICT-processed SMILES ClO profiles for the daytime mid-latitude condition. They concluded that systematic and random errors of 10–35 pptv and 30–40 pptv, respectively, are to be expected for each single retrieval of SMILES ClO at 30–50 km. For the mesosphere above 60 km (pressure  $\leq 0.1$  hPa), the error is dominated by the measurement error

### SMILES ClO comparison

H. Sagawa et al.

Title Page

Abstract

Introduction

Conclusions

References

Tables

Figures

◀

▶

◀

▶

Back

Close

Full Screen / Esc

Printer-friendly Version

Interactive Discussion



**SMILES CIO  
comparison**

H. Sagawa et al.

[Title Page](#)[Abstract](#)[Introduction](#)[Conclusions](#)[References](#)[Tables](#)[Figures](#)[◀](#)[▶](#)[◀](#)[▶](#)[Back](#)[Close](#)[Full Screen / Esc](#)[Printer-friendly Version](#)[Interactive Discussion](#)

due to statistical measurement noise and the smoothing error introduced by the inversion analysis, resulting in the total error of 50–150 pptv. This error can be reduced to some extent by averaging several measurements at the expense of the spatial and temporal resolutions. Averaging 100 profiles measured for the mesosphere can reduce the expected error to the systematic error limit (5 pptv at 0.1 hPa), which is attributed to bias uncertainties in the forward model parameters, specifically the spectroscopic parameters and instruments modeling.

In association with the error analysis by Sato et al. (2012), we intend in this paper to evaluate the quality of the SMILES CIO data generated by the NICT level-2 processing by comparing with those obtained by the following instruments: Aura MLS, Odin SMR, Envisat MIPAS, TELIS and the balloon-borne MIPAS (MIPAS-B). We also compare the NICT-generated data with the results from the SMILES operational level-2 processing developed by the Japan Aerospace Exploration Agency (JAXA). Comparisons with chemical model outputs are beyond the scope of this paper, but Khosravi et al. (2012) compared the CIO diurnal variations obtained by SMILES with their 1-D photochemical model and showed a general good agreement in terms of the relative amplitude of the diurnal cycle.

This paper is organized as follows. The SMILES instrumentation and retrieval procedure are described in Sect. 2. In Sect. 3, the results obtained using the NICT level-2 processing are compared with those derived from the JAXA level-2 chain. Comparisons with other instruments are made in Sect. 4. Finally we summarize the key points in Sect. 5.

## 2 JEM/SMILES

### 2.1 Platform

SMILES was launched on 11 September 2009 and attached to the JEM on the ISS. Scientific measurements of trace gases using SMILES began on 12 October 2009 and

**SMILES CIO  
comparison**

H. Sagawa et al.

[Title Page](#)[Abstract](#)[Introduction](#)[Conclusions](#)[References](#)[Tables](#)[Figures](#)[◀](#)[▶](#)[◀](#)[▶](#)[Back](#)[Close](#)[Full Screen / Esc](#)[Printer-friendly Version](#)[Interactive Discussion](#)

continued until 21 April 2010, when its submillimeter-wave local oscillator failed. The ISS is on a non sun-synchronous circular orbit with an inclination angle of  $51.6^\circ$  to the equator. The SMILES instrument was attached to the JEM with an orientation enabling its antenna field-of-view (FOV) to point in a  $45^\circ$  direction leftward from the ISS orbital motion. The latitudinal coverage of the SMILES observations was nominally between  $65^\circ$  N and  $38^\circ$  S. On days when the ISS was rotated by  $180^\circ$  around its yaw axis, SMILES observation latitude range shifted towards the Southern Hemisphere. The ISS orbit period is  $\sim 91$  min and the local time of the sub-ISS (nadir) point precesses with a full 24 h shift after a 1–2 months period. This enabled SMILES to observe the atmosphere under various local solar times.

Figure 1 shows the time evolution of the sampling density of CIO measured by SMILES under different solar zenith angle (SZA) conditions and for different latitudinal ranges. There were no CIO measurements during December 2009 due to the instrumental configuration. The measurement density increases at both the northern and southern edges of the covered latitudes, where the ISS orbit shifts from ascending to descending. The plots in Fig. 1 illustrate that the sampling density and SZAs for each observation point varied significantly with the season and the latitude. An accumulation of SMILES data over several seasons without any special consideration would result in integrated data reflecting the inhomogeneous contributions from various SZA conditions. Such ISS-orbit induced characteristics should be kept in mind when observing short-lived species like CIO.

## 2.2 SMILES CIO observations

SMILES observes atmospheric emissions in limb-viewing mode via vertically scanning in a tangent height range from  $< 10$  km to  $> 60$  km. One vertical scan is conducted every 29.5 s, and one spectrum is obtained over 0.47 s data integration. The number of measurements (scans) is about 100 points per one cycle of the ISS orbit, which yields a nominal sampling density about 1630 points per day. SMILES is operated in the specific frequency ranges: 624.32–625.52, 625.12–626.32, and

**SMILES CIO  
comparison**

H. Sagawa et al.

Title Page

Abstract

Introduction

Conclusions

References

Tables

Figures

◀

▶

◀

▶

Back

Close

Full Screen / Esc

Printer-friendly Version

Interactive Discussion



649.12–650.32 GHz (referred to Band-A, -B, and -C, respectively). The CIO transitions ( $J = 35/2\text{--}33/2$ ) at 649.445 and 649.451 GHz are observed in the Band-C configuration. The 40 cm  $\times$  20 cm aperture of SMILES main reflector gives an instantaneous FOV of  $0.089^\circ$  (in elevation) in full width at half maximum (FWHM; corresponding to  $\sim 3$  km at the tangent point). The main reflector vertically scans the atmospheric limb at a rate of  $0.009375^\circ$  per 1/12 s, so the actual FOV for the 0.47 s-integrated measurement is a convolution of about six single FOVs. The submillimeter-wave signal is detected by the superconducting heterodyne receiver system which consists of two superconductor-insulator-superconductor (SIS) mixers associated to high electron mobility transistors (HEMT) amplifiers, and is then spectrally resolved by two Acousto-Optical Spectrometers (AOS). The two AOSs detect Band-A, B, or C separately, enabling SMILES to observe two of the three bands simultaneously. Except for December 2009, when Band-C was not operated, the Band-C operation accounts for about 70 % of the total measurements (see Fig. 3 of Kikuchi et al., 2010). The frequency resolution of both AOSs is  $\sim 1.2$  MHz at FWHM with a sampling step of  $\sim 0.8$  MHz. The in-orbit system temperature of SMILES reached as low as  $\sim 350$  K (Ochiai et al., 2010) and the effective noise rms level was  $\sim 0.5$  K for one AOS channel (0.47 s integration).

The physical parameters (called the level-2 products) are derived from the SMILES measurement spectra by solving the inverse problem. The operational level-2 product of SMILES measurement is processed by JAXA (e.g. Kikuchi et al., 2010; Suzuki et al., 2012). NICT developed another level-2 processing chain in order to investigate new alternatives for inversion algorithm (Baron et al., 2011). These products are called the “SMILES NICT level-2 products” and are the data products considered in this study. Version 2.1.5 of the SMILES NICT level-2 product (hereafter denoted NICT v2.1.5 in this paper) was reduced from the calibrated spectra of version 007. The NICT v2.1.5 processing chain employs a least-squares method involving a priori constraints (e.g. Rodgers, 1976, 1990, 2000). A vertical profile of the CIO volume mixing ratio (VMR) was derived for each scan using a spectral bandwidth of 400 MHz centered on the CIO

line. Further details about the inversion methodology of NICT-level-2 processing are found in the papers by Baron et al. (2011) and Sato et al. (2012).

Figure 2 shows examples of the ClO spectra from a limb scan measured during daytime at a low latitude (18.9° S) and the VMR profile retrieved from that specific measurement. The quality of the retrieval can be assessed by considering the goodness of the fit as reported by the chi-squared statistics  $\chi^2$  after the retrieval, the averaging kernels, and the measurement response  $m$ . The definition of  $\chi^2$  in this paper is the summation of the squared and variance-weighted residual terms between the best-fitting spectra and the measurements as well as the deviation of the retrieved state from the a priori state, both normalized by numbers of measurements and retrieval parameters (see Eq. 2 given by Baron et al., 2011). Typical values of  $\chi^2$  for the SMILES NICT ClO profiles are around 0.5–0.8. Here,  $\chi^2$  being smaller than unity is because of the overestimation of the measurement noise (Baron et al., 2011). Averaging kernels describe the sensitivity of the retrieved ClO abundance to the true state of the atmosphere. Their vertical spread is used as an indication of the vertical resolution of the retrievals. The measurement response, which is the sum of the absolute values of elements of each averaging kernel, indicates the effect of the a priori state on the retrieved information (e.g. Baron et al., 2002; Merino et al., 2002). Hereafter, we use relatively soft constraints of  $\chi^2 \leq 0.8$  and  $0.8 \leq m \leq 1.2$  as data selection thresholds in order to exclude extreme outliers. By applying this data selection, approximately 12 % of the total measurements were discarded due to the  $\chi^2$  threshold. For a single-scan measurement, the SMILES NICT v2.1.5 ClO product has a satisfactory measurement sensitivity at altitudes of  $\sim 17$ –80 km (corresponding to a pressure range of  $\sim 80$ –0.01 hPa) with a typical vertical resolution of 3.5–13 km.

Figure 3 shows an example of ClO diurnal variation in the middle stratosphere (10 hPa) observed with SMILES. Two months of observations (January and February 2010) for the equatorial region were zonally averaged using a 1-h local time bin. Each vertical bar represents the  $1\text{-}\sigma$  standard deviation of the measurements for each bin. For comparison, the ClO abundances obtained by Aura MLS, Odin SMR, and Envisat

**SMILES ClO  
comparison**

H. Sagawa et al.

Title Page

Abstract

Introduction

Conclusions

References

Tables

Figures

◀

▶

◀

▶

Back

Close

Full Screen / Esc

Printer-friendly Version

Interactive Discussion



**SMILES CIO  
comparison**

H. Sagawa et al.

[Title Page](#)[Abstract](#)[Introduction](#)[Conclusions](#)[References](#)[Tables](#)[Figures](#)[◀](#)[▶](#)[◀](#)[▶](#)[Back](#)[Close](#)[Full Screen / Esc](#)[Printer-friendly Version](#)[Interactive Discussion](#)

MIPAS for the same period are shown. Data from these other instruments are described in detail later (Sect. 4), as are the difference in the CIO VMRs. Here we note the small standard deviations ( $\sim 6$  pptv and 15 pptv for nighttime and daytime, respectively) for the SMILES CIO profiles that indicate the good sensitivity of SMILES observations. The lower panel of Fig. 3 shows the local-time evolution of the observed points over the two months. These results clearly show the benefit for SMILES of a non sun-synchronous orbit: while the other instruments are onboard sun-synchronous satellites thus measuring only at fixed local times, SMILES samples a broad range of local time allowing the instrument to effectively observe the diurnal variations of CIO.

**2.3 Error analysis for the SMILES NICT CIO profiles**

The systematic (bias) and random errors of the SMILES NICT v2.1.5 CIO product were investigated by Sato et al. (2012). They estimated the systematic error to be 35 pptv for the CIO peak altitudes (around 2–4 hPa) for typical mid-latitude daytime CIO abundances. This systematic error was dominated by the error due to an uncertainty in the pressure broadening parameter of the CIO spectral line. The previously reported known analytical problems for the presented version of the NICT CIO product are as follows: (1) the vertical movement of the SMILES FOV during a single spectrum integration of 0.47 s was ignored in the forward model; (2) an ideal rejection rate for the image side band signal was assumed instead of using the actual characteristics of the sideband separation filter. Sato et al. (2012) showed that systematic errors of  $\sim 2$ –4 and  $\sim 0.5$  pptv were introduced at 2–4 hPa in the CIO profiles when ignoring the FOV vertical movement and the sideband filter characteristic, respectively, which are regarded as rather minor contributors to the total systematic error.

Here we performed an additional error analysis on the SMILES CIO data for two specific measurement conditions: nighttime and chlorine-activated polar air. The reference CIO VMR profiles used in the simulation are shown in the left plot of Fig. 4. The error sources considered in this study are summarized in Table 1. These sources were selected as the most significant systematic error sources in the forward model according

SMILES ClO  
comparison

H. Sagawa et al.

Title Page

Abstract

Introduction

Conclusions

References

Tables

Figures

◀

▶

◀

▶

Back

Close

Full Screen / Esc

Printer-friendly Version

Interactive Discussion



to the previous work by Sato et al. (2012). In addition to the error sources they had investigated, we introduced a spectroscopic parameter error due to the uncertainty on line position. This error was evaluated by testing retrievals with two values for the line positions of the ClO doublet spectra: one from the JPL spectroscopic catalogue (Pickett et al., 1998) (649.445040 and 649.451170 GHz), which was used in the original NICT v2.1.5 processing, and the other from the laboratory measurements of Oh and Cohen (1994) (649.445250 and 649.451072 GHz). The null-space error also contributes to the systematic errors in certain conditions. NICT v2.1.5 processing uses fixed a priori values for ClO based on a typical mid-latitude daytime profile. This can introduce a systematic bias for ClO retrievals under nighttime and chlorine-activated conditions where, in practice, ClO VMRs differ significantly from the assumed a priori daytime values. This impact was estimated in this study by calculating  $(\mathbf{A} - \mathbf{I})(\mathbf{x}_{\text{ref}} - \mathbf{x}_{\text{a priori}})$ , where  $\mathbf{A}$  is the averaging kernel matrix,  $\mathbf{I}$  is the identity matrix,  $\mathbf{x}_{\text{a priori}}$  is the ClO a priori VMR used in the NICT v2.1.5 processing, and  $\mathbf{x}_{\text{ref}}$  is the reference ClO profile assumed in the error analysis simulations. Since we added these error sources, we recomputed the error for the mid-latitude daytime conditions and checked the consistency with the previous results of Sato et al. (2012). Note that the null-space error was regarded as a random error for the daytime ClO retrievals, as discussed by Sato et al. (2012).

The right panel of Fig. 4 shows the estimated systematic errors for three typical ClO profiles. For each profile, the considered systematic errors were divided into four components: error due to uncertainties in the spectroscopic parameters of ClO, error from other species in the radiative transfer model, error due to the uncertainty on the instrumental description in the forward model, including errors on the spectral gain calibration, and error from the use of a fixed a priori profile. The total systematic error was calculated as the root-sum-square (rss) of individual error sources. From the simulation results, we obtained the systematic errors ( $1-\sigma$  standard deviation of the bias uncertainty) shown in Table 2. In Table 2 we also included the  $1-\sigma$  precision (random error) for a single-scan profile. For the daytime mid-latitude condition the systematic error was estimated as 5–10 pptv, 35 pptv, and 5–10 pptv for the lower stratosphere (at pressure

**SMILES CIO  
comparison**

H. Sagawa et al.

[Title Page](#)[Abstract](#)[Introduction](#)[Conclusions](#)[References](#)[Tables](#)[Figures](#)[◀](#)[▶](#)[◀](#)[▶](#)[Back](#)[Close](#)[Full Screen / Esc](#)[Printer-friendly Version](#)[Interactive Discussion](#)

80–20 hPa), the CIO peak altitude ( $\sim 4$  hPa), and the upper stratosphere/lower mesosphere (pressure  $\leq 0.5$  hPa). These values are consistent with those presented by Sato et al. (2012), except for the lower mesosphere where the additional error due to the spectroscopic parameter is newly considered. For the nighttime mid-latitude condition systematic errors of 8 pptv and 3–15 pptv were estimated for the CIO nighttime peak altitude ( $\sim 2$  hPa) and the upper stratosphere/lower mesosphere (pressure  $\leq 0.5$  hPa), respectively. In the lower stratosphere (at pressure 80–20 hPa), our estimated systematic error was less than 4 pptv. However, the actual SMILES NICT v2.1.5 CIO profiles have a more significant negative bias about  $-30$  pptv at 80 hPa (see details in Sect. 4.2.1). This implies that there are unimplemented or underestimated bias errors in the presented simulation, and for the scientific use of the SMILES NICT v2.1.5 data, we should take this observed negative bias into account. The systematic errors for the measurements of CIO activation in polar vortex were estimated to be 80–320 ppbv (at pressure range of  $\sim 30$ –80 hPa) assuming an enhanced CIO abundance of 1.0 ppbv, which mostly comes from the a priori contamination. This corresponds to a 10–35% relative error.

### 3 Methodology of comparison

The SMILES NICT v2.1.5 CIO profiles were compared to (1) the SMILES CIO profiles processed by the JAXA level-2 chain (version 2.1), (2) the Aura MLS version 3.3 CIO profiles, (3) the Odin SMR CIO profiles from the version 2.1 of Chalmers level-2 processing, (4) the Envisat MIPAS IMK/IAA data version V5R\_CIO\_220, and (5) the TELIS and MIPAS-B balloon-borne measurements. Comparison-(1) enables us to discern differences between the processing algorithms, since both the NICT and JAXA SMILES CIO profiles were processed from the same calibrated radiance (level-1B product version 007). The target for (2) and (3) is a comparison of the coincident geolocation measurements with those of satellite-based measurements for validating the sensitivity of SMILES at various local times in the middle stratosphere. The target for (4) is

**SMILES ClO  
comparison**

H. Sagawa et al.

Title Page

Abstract

Introduction

Conclusions

References

Tables

Figures

◀

▶

◀

▶

Back

Close

Full Screen / Esc

Printer-friendly Version

Interactive Discussion



a comparison of the latitudinal distribution of ClO in the lower and middle stratosphere by calculating a median of the zonally accumulated dataset instead of finding coincident observations. This was because of the large difference in the measurement sensitivities of SMILES and MIPAS. Comparison-(5) with TELIS and MIPAS-B which flew within the northern polar vortex, is aimed at evaluating the performance of SMILES ClO measurements under conditions of strong chlorine activation in the lower stratosphere. Further information on each comparison dataset is summarized in the following subsections, followed by the results of the comparison with the SMILES NICT product. We did not include any datasets from ground-based observations in this paper because of the relatively large difference in the sensitivity.

Comparisons-(1–3 and 5) were performed using the individual profile comparison approach, which has worked well for comparing various remote sensing observations (e.g. Dupuy et al., 2009). We searched all coincident measurements profiles (i.e. quasi-simultaneous observations in very close collocation) between the SMILES and comparison datasets and then calculated the representative values of their differences to obtain an average absolute difference profile. To be less sensitive to outliers, we use the median statistic instead of the mean statistic to derive the average state. The variability of the compared datasets was estimated by calculating the median absolute deviation (hereafter abbreviated to MAD) values. The average relative difference was obtained by first calculating the individual relative differences on the basis of the ratio of the difference to the mean of the compared pair of ClO profiles. Then we took the median of those relative differences over the full set of coincident pairs.

As discussed by Rodgers and Connor (2003), the difference in the averaging kernels should be taken into account when comparing the results derived from different remote sensing instruments. One of the most significant impacts of the different averaging kernels appears as the difference in vertical resolutions. Figure 5 shows the typical vertical resolution of ClO profiles from different measurements used in this study. It is shown that, in the middle stratosphere the SMILES NICT v2.1.5 profiles have similar vertical resolutions with those of the SMILES JAXA level-2 chain, MLS, and SMR:

## SMILES CIO comparison

H. Sagawa et al.

Title Page

Abstract

Introduction

Conclusions

References

Tables

Figures

◀

▶

◀

▶

Back

Close

Full Screen / Esc

Printer-friendly Version

Interactive Discussion



the vertical resolution of SMILES NICT v2.1.5 is 3.5–5 km at a pressure range of ~30–1 hPa and 5–8 km at 1–0.1 hPa. It is 3–5 km at 200–0.1 hPa for the SMILES JAXA level-2 product; 3–4.5 km at 147–1 hPa for Aura MLS (Livesey et al., 2011); and 2.5–3 km at 100–1 hPa for Odin SMR (Urban et al., 2006). However, in the lower stratosphere (pressure  $\geq 30$  hPa) the vertical resolution of SMILES NICT v2.1.5 starts degrading to 5–8 km, and is the lowest resolution in the datasets considered in this study. In fact, the CIO profile measured by TELIS has a vertical resolution of 2–3 km in the lower stratosphere, which is more than twice better than that of the SMILES NICT v2.1.5 profiles, because it was situated within the atmosphere, which helps in significantly reducing the FOV of the measurement. Such differences in the averaging kernels strongly affect the comparison of the lower stratospheric CIO enhancement in the polar vortex. Therefore, when CIO profiles from the polar vortex were targeted in the comparison (i.e. the comparison between SMILES NICT processing and the JAXA processing in Sect. 4.2.2, and the comparisons between SMILES and TELIS, MIPAS-B in Sect. 5.4), we convolved the averaging kernels of the SMILES NICT v2.1.5 CIO profiles,  $\mathbf{A}$ , on the higher-resolution profiles using the following function:

$$\mathbf{x}_{\text{smooth}} = \mathbf{A}\mathbf{x}_{\text{highres}} + (\mathbf{I} - \mathbf{A})\mathbf{x}_{\text{a priori}} \quad (1)$$

$\mathbf{x}_{\text{highres}}$  represents the retrieved CIO profile from the higher-vertical resolution instrument, and  $\mathbf{x}_{\text{smooth}}$  is the same but after convolution of the SMILES NICT v2.1.5 averaging kernels.  $\mathbf{x}_{\text{a priori}}$  is the a priori profile used in the SMILES NICT v2.1.5 processing. For MIPAS-B the vertical resolution is comparable to that of TELIS, however the CIO signals are weak in the observed infrared region causing relatively low amplitudes of the averaging kernels (peak values of the averaging kernels are smaller than 0.4 at altitudes above 20 km). Therefore, when comparing the SMILES profile with MIPAS-B, the averaging kernel matrices of both SMILES and MIPAS-B were considered: the SMILES averaging kernels were convolved on MIPAS-B CIO profile and the MIPAS-B averaging kernels were convolved on SMILES CIO profile. This convolution was applied to each

individual profile in before taking the median of VMRs or calculating the differences of coincident profiles.

For the SMILES-MIPAS comparison-(4), we calculated the zonally averaged latitudinal CIO distributions of the two datasets. The CIO distributions from both datasets were gridded in a latitude and pressure plane. Similarly to the approach applied to the individual profile comparison, we used median values instead of mean to calculate the representative VMRs for each pixel. The variation of the measurements at each pixel was examined by calculating median absolute deviations. The vertical resolution of MIPAS is 3–8 km at 100–10 hPa (Fig. 5), having its better resolution in the lower stratosphere where that of SMILES NICT v2.1.5 degrades. In order to solve this discrepancy in the vertical resolution the smoothing of VMR profiles was applied to both datasets, i.e. the SMILES CIO profile was smoothed to the MIPAS vertical resolution and vice versa. The smoothing was done by using triangular functions of full width at the base equal to the vertical resolution.

## 4 Comparison of NICT v2.1.5 and JAXA level-2 profiles

### 4.1 Differences in the processing algorithms

We performed a SMILES-internal comparison between the NICT v2.1.5 product and the JAXA level-2 product (version 2.1, 007-08-0310)<sup>1</sup>. Both the SMILES NICT v2.1.5 and JAXA level-2 processings are based on the least-squares method using regularizations (Baron et al., 2011; Suzuki et al., 2012). There are six major differences in the forward model parameters and also in the retrieval configurations:

1. Spectral range of the measurements used in the inversion calculation: the JAXA level-2 processing uses the full bandwidth of the Band-C spectrum,

<sup>1</sup>Documentation is available at [http://smiles.isas.jaxa.jp/access/SMILES\\_L2\\_product\\_v2-1\\_release\\_note.pdf](http://smiles.isas.jaxa.jp/access/SMILES_L2_product_v2-1_release_note.pdf).

## SMILES CIO comparison

H. Sagawa et al.

Title Page

Abstract

Introduction

Conclusions

References

Tables

Figures

◀

▶

◀

▶

Back

Close

Full Screen / Esc

Printer-friendly Version

Interactive Discussion



**SMILES ClO comparison**

H. Sagawa et al.

Title Page

Abstract

Introduction

Conclusions

References

Tables

Figures

◀

▶

◀

▶

Back

Close

Full Screen / Esc

Printer-friendly Version

Interactive Discussion



simultaneously retrieving ClO and other trace gases such as HO<sub>2</sub>, while the NICT v2.1.5 processing uses a limited bandwidth (400 MHz) centered on the ClO line. As discussed by Baron et al. (2011), using a narrower bandwidth degrades the sensitivity to lower altitudes since the information at those low altitudes, i.e. high pressure levels, is spread out in the far wings of the ClO emission line.

2. Correction of the AOS frequency offset: AOS frequencies are corrected with an offset parameter through the retrieval calculations in the NICT v2.1.5 processing, while they are fixed in the JAXA v2.1 processing.
3. Spectroscopic parameters used in the forward model, in particular, the line frequency  $\nu_0$ , the air broadening coefficient  $\gamma_{\text{air}}$ , and its temperature dependence  $n_{\text{air}}$ : the JAXA v2.1 processing uses coefficients based on Oh and Cohen (1994) ( $\nu_0 = 649.445250$  and  $649.451072$  MHz,  $\gamma_{\text{air}} = 2.11$  MHz mbar<sup>-1</sup>, i.e.  $2.81$  MHz Torr<sup>-1</sup>, and  $n_{\text{air}} = 0.85$ ), while the NICT v2.1.5 processing uses the JPL catalog frequencies (Pickett et al., 1998) and original values for the air broadening coefficients ( $\nu_0 = 649.445040$  and  $649.451170$  MHz,  $\gamma_{\text{air}} = 2.86$  MHz Torr<sup>-1</sup>, and  $n_{\text{air}} = 0.77$ ; see details in the paper by Baron et al., 2011).
4. ClO a priori profiles: the JAXA level-2 processing employs the monthly, latitudinal, day-night-separated mean of the MLS v2.2 product. The NICT v2.1.5 processing uses a single common profile for all observations. The a priori temperature and pressure profiles also differ between the two level-2 processings.
5. Correlation length of the retrieval vertical layers (i.e. non-diagonal components of the a priori covariance matrix): 10 and 6 km are used in the JAXA v2.1 and NICT v2.1.5 processings, respectively.
6. Correction approach of the LOS elevation angles (i.e. tangent point heights): both processors retrieve an offset parameter for the LOS elevation angles within a single scan but in a different way. The JAXA level-2 processing uses the result of

tangent point retrieval from Band-A or -B, which contains the strong O<sub>3</sub> transition at 625.371 GHz, as a priori value for retrieving the LOS elevation angle offset of the Band-C spectra. In contrast, the NICT v2.1.5 processing does not link the information from Band-A or -B to the retrieval of Band-C in order to avoid propagating any systematic errors between the two bands. It retrieves an LOS elevation angle offset from the CIO spectra, for which most of the information comes from the continuum baseline.

As shown in Fig. 5, the vertical resolution of the JAXA CIO product is slightly better than those of NICT v2.1.5.

## 4.2 Results

### 4.2.1 Comparison at the middle and low latitudes

Figure 6 shows the comparison between the CIO profiles from NICT v2.1.5 and the JAXA level-2 v2.1 products for equatorial latitudes (20° S–20° N) in February and April 2010. We compared the day and night profiles separately by selecting the profiles with SZAs  $\leq 80^\circ$  and  $\geq 100^\circ$ , respectively. There were 4539 and 5456 measurements for the day and night conditions, respectively. The left two panels show the median VMRs of the selected CIO profiles, for the day and night cases, with 1-MAD values (dashed lines). Medians of the absolute and relative differences are shown in the right panels. The dotted lines around the absolute difference profiles correspond to the 1-MAD of the individual absolute difference of each pair. The relative difference is plotted with a focus on the altitude range where the CIO concentration is not too small, i.e. at altitudes around 0.5–20 hPa and 0.05–3 hPa for the day and night profiles, respectively.

At the CIO peak altitudes (pressure levels of 4 and 2 hPa for day and night, respectively), the NICT v2.1.5 CIO profile shows larger VMRs than the JAXA-processed one; in detail, the differences are 15 and 10 pptv (or about 5%) for day and night, respectively. Although these discrepancies between the daytime and nighttime profiles are within or comparable to the estimated 1- $\sigma$  bias uncertainty of the v2.1.5 product, we

Title Page

Abstract

Introduction

Conclusions

References

Tables

Figures

◀

▶

◀

▶

Back

Close

Full Screen / Esc

Printer-friendly Version

Interactive Discussion



**SMILES CIO  
comparison**

H. Sagawa et al.

[Title Page](#)[Abstract](#)[Introduction](#)[Conclusions](#)[References](#)[Tables](#)[Figures](#)[◀](#)[▶](#)[◀](#)[▶](#)[Back](#)[Close](#)[Full Screen / Esc](#)[Printer-friendly Version](#)[Interactive Discussion](#)

are interested in knowing whether such discrepancies can be explained by the use of different spectroscopic parameters in the two forward models. To investigate this, we randomly selected a sample of 200 SMILES level-1B scans from the equatorial daytime measurements for one day (4 January 2010), and processed them using the spectroscopic parameters of the NICT v2.1.5 forward model and using those of the JAXA level-2 processing. By replacing the spectroscopic parameters with those used in the JAXA processing, the CIO VMR was decreased by  $\sim 7$  pptv at 1–2 hPa but no significant change was observed at 4 hPa where we have seen the largest difference between the NICT v2.1.5 and the JAXA v2.1 CIO products. This suggests that the difference between the NICT and the JAXA CIO profiles is not solely due to the different spectroscopic parameters, but is rather a result of other factors that remain to be identified. Further investigation of this difference is currently under way, using a new version of the calibrated spectra. It should be mentioned that we saw a significant improvement in the residual of the best-fit spectra when the line positions from Oh and Cohen (1994) were used. Such an error on the line position is especially significant for observations of the nighttime mesosphere where an enhancement of the CIO is observed.

In the nighttime lower stratosphere (pressure  $\geq 30$  hPa) where CIO abundances are known to be nearly zero outside the polar region, the NICT v2.1.5 CIO profiles show negative VMRs of about  $-30$  pptv. As mentioned in Sect. 2.3, this negative bias is slightly larger than our estimated bias uncertainty. The increase of 1-MAD values, i.e. increase of variability of the NICT v2.1.5 CIO data at those altitudes, indicates that the retrieval processing has some problems. The reason for this negative bias is thought to be the limited spectral bandwidth used in the NICT processing. Using such a relatively narrow bandwidth introduces a contamination from other broadened spectral lines which cannot be distinguished from the CIO spectral signal. The NICT level-2 processing team is now working to solve this issue by implementing analyses based on the full bandwidth of SMILES spectra.

We also examined latitudinal and seasonal variations of the difference between the NICT v2.1.5 and JAXA v2.1 CIO profiles. In both daytime and nighttime conditions,



features outside the bandwidth and also a relatively larger contamination from the incorrect a priori CIO profile. Similarly to the negative bias in the nighttime mid-latitude retrievals, this problem will be considered in the next version of the NICT level-2 processing. The characteristics of the CIO profiles under polar vortex conditions will be discussed further when we compare the SMILES measurements to those of TELIS and MIPAS-B (Sect. 5.4).

## 5 Comparison with other instruments datasets

### 5.1 Comparison with Aura MLS v3.3 data

The Microwave Limb Sounder (MLS) onboard NASA's Earth Observing System (EOS) Aura satellite has been operating since 2004 (Waters et al., 2006). The satellite was launched into a near polar sun-synchronous orbit with the equator crossing local times of 13:45 (ascending) and 01:45 (descending). Aura MLS observes CIO with a radiometer centered at 640 GHz; that is the same CIO transition that SMILES measures. The frequency resolution is 6 MHz at the line center channels and increases to 96 MHz at the band edge. The system noise temperature is  $\sim 4200$  K in double side-band receiver mode, and the typical rms noise level for a single spectrum (integration time of 1/6 s) is 4.2 K for a 6 MHz-resolution channel (Waters et al., 2006).

The CIO abundances were retrieved from the MLS measurement data using the optimal estimation method. The retrieval algorithm used was that reported by Livesey et al. (2006). A remarkable feature of their data processing is that not only the vertical profile information of the CIO, but also its horizontal distribution, is retrieved by combining consecutive limb scan measurements (the FOV of MLS is set in the forward direction of the Aura orbital motion, so consecutive measurements contain information from partially overlapping air masses). The observed data has been reprocessed using version 3.3 of the algorithm since 2011. In this version, the useful range for the CIO profile is defined as 147 to 1 hPa (vertical resolution of  $\sim 3$ –4.5 km) with a precision of

Title Page

Abstract

Introduction

Conclusions

References

Tables

Figures

◀

▶

◀

▶

Back

Close

Full Screen / Esc

Printer-friendly Version

Interactive Discussion



~ 0.1–0.3 ppbv for a single scan (Livesey et al., 2011). The systematic uncertainty was estimated to be 0.025 ppbv at 15–1 hPa.

Santee et al. (2008) performed an intensive validation study for a previous version, version 2.2, of the Aura MLS CIO product. Their study showed that both the height of the peak in CIO profiles and its amplitude are well determined in the Aura MLS measurements, which makes the MLS data one of the best comparison partners for the SMILES data. For the lower stratosphere (typically pressures larger than 22 hPa) significant negative VMRs were found for the MLS dataset in both daytime and nighttime profiles. This negative bias problem was improved in the version 3.3 processing although altitude- and latitude-dependent biases of about  $-0.1$  to  $+0.6$  ppbv at pressures higher than 68 hPa still need to be accounted for. The recommended correction values reported by the MLS team can be found in Livesey et al. (2011) and in the documentation on the MLS website<sup>2</sup>.

Figure 8 shows comparison results between the SMILES and MLS CIO measurements. Coincidence measurements were searched for over the whole SMILES observation period in the low and middle latitude region (latitudes lower than  $60^\circ$ ). We defined three criteria for determining coincidence: observation points are closer than 100 km, observation time difference is smaller than 1 h, and the SZA difference is less than  $3^\circ$ . Using these criteria, we found 578 and 418 coincidences for daytime ( $SZA \leq 80^\circ$ ) and nighttime ( $SZA \geq 100^\circ$ ), respectively. The solid lines on the average VMR profiles for the MLS products are those before bias correction. There is a clear negative bias for the altitudes where pressure is larger than  $\sim 50$  hPa. We applied the bias corrections suggested by the MLS team; the corrected VMRs are shown as symbols on the graph. After this correction, the daytime CIO profiles from both the SMILES and MLS showed a good agreement for the considered altitude range (100–1 hPa). The SMILES CIO VMR was smaller than the MLS one by  $\sim 0.04$  ppbv (10%) at the daytime peak altitude. This difference is within the combined (0.035 ppbv and 0.025 ppbv for SMILES and MLS, respectively) bias uncertainty.

<sup>2</sup>[http://mls.jpl.nasa.gov/data/MLS\\_v3-3\\_CIO\\_BiasCorrection.txt](http://mls.jpl.nasa.gov/data/MLS_v3-3_CIO_BiasCorrection.txt)

SMILES CIO  
comparison

H. Sagawa et al.

Title Page

Abstract

Introduction

Conclusions

References

Tables

Figures

◀

▶

◀

▶

Back

Close

Full Screen / Esc

Printer-friendly Version

Interactive Discussion



**SMILES CIO comparison**

H. Sagawa et al.

[Title Page](#)[Abstract](#)[Introduction](#)[Conclusions](#)[References](#)[Tables](#)[Figures](#)[◀](#)[▶](#)[◀](#)[▶](#)[Back](#)[Close](#)[Full Screen / Esc](#)[Printer-friendly Version](#)[Interactive Discussion](#)

For the nighttime case, the SMILES CIO data also showed negative VMRs for the lower stratosphere ( $\sim -0.03$  ppbv), as already pointed out by the SMILES-internal comparison. Except for this altitude region, the SMILES CIO measurements have nearly zero 1-MAD values, confirming that there is no CIO at these altitudes during the nighttime. This is a clear indication of the high sensitivity of SMILES measurement.

**5.2 Comparison with Odin SMR v2.1 data**

The Sub-Millimetre Radiometer, SMR, onboard the Odin satellite has been measuring stratospheric CIO since 2001 (Murtagh et al., 2002). Odin, an astronomical and aeronautical satellite mission by Sweden, France, Canada, and Finland has a circular sun-synchronous orbit (inclination angle of  $97.8^\circ$ ), with equator-crossing local times of about 18:00 (ascending) and 06:00 (descending), respectively. SMR has a 1.1 m diameter reflector that is used to observe the atmospheric limb emission. The receiver consists of four single-sideband Schottky diode heterodyne mixers operating in the frequency range of 486–581 GHz. The CIO transitions are observed at 501.3 GHz with a typical receiver noise temperature of 3000 K (single side-band).

The level-2 data processing of Odin SMR was divided into an operational processing at Chalmers University in Sweden and a research processing named CTSO (Chaîne de Traitement Scientifique Odin) developed by a French team, though the CTSO processing chain is no longer operated now. We used the recommended Chalmers operational CIO product, version 2.1, for comparison with the SMILES data. The bias uncertainty and the random errors were estimated to be smaller than 0.1 ppbv and 0.15 ppbv, respectively (Urban et al., 2006). These data were compared with the MLS CIO profiles (Santee et al., 2008; Livesey et al., 2011), which showed a good agreement in the middle stratosphere (pressure  $\leq 46$  hPa) having only a small difference of  $\sim 0.05$  ppbv (SMR Chalmers-v2.1 VMRs are smaller than MLS) around 10 hPa. For the lower stratosphere, it was suggested that the SMR profiles may have a positive bias of 0.1 to 0.2 ppbv for the nighttime measurements outside the polar vortex, when CIO abundances become smaller than the instrument sensitivity limit (Barret et al., 2006).

**SMILES CIO  
comparison**

H. Sagawa et al.

Title Page

Abstract

Introduction

Conclusions

References

Tables

Figures

◀

▶

◀

▶

Back

Close

Full Screen / Esc

Printer-friendly Version

Interactive Discussion



In this study, we loosened the geolocation criterion for coincidence determination to 300 km due to the relatively small data sampling density of the Odin SMR measurements ( $\leq 975$  per day). The Odin SMR CIO measurements are carried out shortly after sunrise and sunset, when the concentration of CIO drastically changes due to photochemistry. Therefore, the criterion for the SZA difference was kept as narrow as it was for the SMILES–MLS comparison. We identified 89 coincidences for the sunrise and sunset data in the low and middle latitudes (latitude  $\leq 60^\circ$ ). Figure 9 shows the median CIO profiles and their differences derived from the coincident pairs of SMILES and SMR data. The difference between SMILES and SMR CIO profiles in the stratosphere is quantitatively consistent with that reported in the previous MLS–SMR comparisons (e.g. see Fig. 3.5.8 of Santee et al., 2008; Livesey et al., 2011). At the CIO peak altitudes ( $\sim 2$  hPa), the SMILES CIO VMR was larger than that of SMR by up to 0.05 ppbv, while in the lower stratosphere (pressure  $\geq 30$  hPa) the SMILES profiles had smaller VMRs by  $\sim 0.1$  ppbv. What is new in our comparison result is the comparison in the lower mesosphere (pressure  $\leq 1$  hPa). Both SMILES and SMR observed the decrease of CIO VMRs with altitude above the 1 hPa level. At the 0.2 hPa level the SMR CIO profiles show unrealistic negative VMRs of  $-0.05$  hPa and therefore we cannot quantitatively conclude whether there is any systematic bias in the SMILES data. It is noted that SMR changes its vertical scanning scheme in the  $\sim 50$ – $70$  km altitude range resulting in a reduction of the vertical resolution, and therefore differences in the data characteristics are expected in this region.

### 5.3 Comparison with Envisat MIPAS V5R\_CIO\_220 data

The Michelson Interferometer for Passive Atmospheric Sounding (MIPAS) onboard ESA's Environmental Satellite (Envisat) is a Fourier transform spectrometer operating in the spectral range of 4.15 to 14.6  $\mu\text{m}$  (Fischer et al., 2008). It observed the atmospheric emission in the limb scanning geometry. The platform had a sun-synchronous orbit with an inclination angle of  $98.55^\circ$ . The equator crossing local times were around 10:00 and 22:00. The observations were performed from July 2002 to April 2012, with

**SMILES ClO  
comparison**

H. Sagawa et al.

Title Page

Abstract

Introduction

Conclusions

References

Tables

Figures

◀

▶

◀

▶

Back

Close

Full Screen / Esc

Printer-friendly Version

Interactive Discussion



a discontinuity between April and December 2004 due to an instrumental anomaly. The observation mode (tangent height sampling of the limb and spectral resolution), which determines the data characteristics, was changed after this discontinuity. The ClO data was retrieved from the weak 1–0 band at 11.8  $\mu\text{m}$  using only P and Q branches, which are free of the overlapping contaminating  $\text{HNO}_3$  emission. Due to major overlap of the ClO lines with those of  $\text{O}_3$  and  $\text{CO}_2$  and the low sensitivity of MIPAS ClO measurements, this species had not been considered as a regular scientific data product in preflight sensitivity studies. Glatthor et al. (2004), however, showed that useful ClO distributions could be derived from MIPAS measurements under conditions of ClO enhancements. The scientifically usable altitude range reported in their paper was 10–30 km, but von Clarmann et al. (2005) have also detected ClO enhancements in the upper stratosphere. In 2004 a technical problem with MIPAS was encountered, and from 2005 until the loss of Envisat in April 2012, MIPAS measured at reduced spectral resolution. Total estimated retrieval errors are dominated by measurement noise, and range from 19 to 385 pptv in the altitude range from 10–30 km, which exceeds the 100 % limit between about 15 and 20 km (von Clarmann et al., 2009). Thus, under normal conditions, i.e. no chlorine activation, single MIPAS ClO profiles are of limited use and averages should be used instead.

We used version V5R\_CIO\_220 of the MIPAS scientific level-2 product processed by the Institute for Meteorology and Climate Research (IMK) at Karlsruhe Institute of Technology, Germany. This is the offline-reprocessing high-spectral-resolution version. The zonal median average of the January–March data for 2010 was calculated by collecting the MIPAS ascending-orbit data, i.e. observations at 10:00 a.m. LT. We used the data from altitudes whose diagonal elements of the averaging kernel matrix were larger than 0.1 (about 12–30 km). The zonal average plots for the SMILES data were generated using the data for the local solar times of 10:00 a.m.  $\pm$  15 min for January–March of 2010. It is worth noting that the SMILES measurements are not regularly distributed in the three-month data accumulation.

**SMILES CIO  
comparison**

H. Sagawa et al.

[Title Page](#)[Abstract](#)[Introduction](#)[Conclusions](#)[References](#)[Tables](#)[Figures](#)[◀](#)[▶](#)[◀](#)[▶](#)[Back](#)[Close](#)[Full Screen / Esc](#)[Printer-friendly Version](#)[Interactive Discussion](#)

Figure 10 shows the composed zonal median distributions and median absolute deviations of the MIPAS and SMILES CIO profiles. The median values were calculated for each latitude–pressure pixel which contains  $\sim 600$ – $1500$  measurements for MIPAS and  $\sim 50$ – $100$  for SMILES. The white dashed line represents the approximate altitude level of 30 km, indicating the typical upper boundary of the usable altitude range of the MIPAS dataset.

Both MIPAS and SMILES distributions exhibit latitudinal variations in daytime stratospheric CIO. The CIO VMR for mid latitudes ( $\sim 40$ – $50^\circ$ ) is greater than that for low latitudes in both datasets. Also the altitude range where the median CIO VMR exceeds 100 pptv agrees fairly well (above 20–30 hPa) outside of the polar region. The SMILES median VMRs at 10 hPa, however, are higher than those of MIPAS by approximately 100 pptv (this was also shown in Fig. 3 in Sect. 2). Considering the good agreement of SMILES CIO VMR with MLS and SMR, and given that the upper limit of MIPAS CIO sensitivity is at  $\sim 10$  hPa, we consider that this difference is likely due to a negative bias of the MIPAS dataset. Note that the day-to-night amplitude of CIO diurnal cycle observed in the MIPAS dataset is about 200 pptv (see Fig. 3) which is in fair agreement with that derived from SMILES (250 pptv).

The mid-latitudinal enhancement of CIO in the lower and middle stratosphere was observed by both instruments. In the lower stratosphere (pressure  $\geq 30$  hPa), the MIPAS zonal average distribution shows an enhancement of CIO in the northern polar vortex air. SMILES was not suitable to clearly catch such a feature due to the limitation of the ISS orbit. Nevertheless, the SMILES data show CIO VMRs of 100 pptv at latitudes higher than  $60^\circ$  N, which is the result of partially measuring the chlorine-activated feature in the polar vortex. When quantitatively comparing the polar CIO enhancements from both datasets, we have to bear in mind that the SMILES dataset shown here is limited to observations around 10:00 a.m. LT. Unlike the MIPAS dataset representing median values of the measurements for almost full period over January–March 2010, the SMILES dataset is not representative of the three months period but is composed of measurements from only 30 January–8 February with a quite inhomogeneous

**SMILES ClO  
comparison**

H. Sagawa et al.

[Title Page](#)[Abstract](#)[Introduction](#)[Conclusions](#)[References](#)[Tables](#)[Figures](#)[◀](#)[▶](#)[◀](#)[▶](#)[Back](#)[Close](#)[Full Screen / Esc](#)[Printer-friendly Version](#)[Interactive Discussion](#)

sampling of the inside/outside of vortex. At these high latitudes there is a large variability of the ClO abundance, as seen in the large 1-MAD value (150 pptv) for the SMILES dataset, which is affected by the displacement of the polar vortex center after a sudden stratospheric warming on 21 January. Under such a condition, a perfect agreement between SMILES and MIPAS VMRs cannot be expected in the polar region. At 50–100 hPa at low latitudes, MIPAS data show unrealistic negative VMRs (–60 pptv). However, as already shown by Glatthor et al. (2004), MIPAS is not sensitive to ClO in such low VMR conditions. While these low sensitivities of MIPAS to ClO impede its use for quantitative ClO validation, the fact that both instruments see similar spatial patterns in the ClO distributions and fairly consistent diurnal variation is encouraging.

**5.4 Comparison with TELIS and MIPAS-B measurements inside the polar vortex**

TELIS, the Terahertz and submillimeter Limb Sounder, is a balloon-borne instrument equipped with cryogenic heterodyne technology similar to SMILES. The balloon-borne Michelson Interferometer for Passive Atmospheric Sounding (MIPAS-B) is an advanced Fourier transform infrared spectrometer specially tailored to operate on a stratospheric balloon gondola. Essential for the balloon instrument is the sophisticated line-of-sight (LOS) stabilization system, which is based on an inertial navigation system and supplemented with an additional star reference system. Both TELIS and MIPAS-B are mounted on the MIPAS-B2 gondola sharing the platform with the mini-DOAS instrument. In this configuration the gondola was launched in three consecutive winters (2009–2011) from Kiruna, Sweden. In this study only the second flight in 2010, when SMILES was operational, is considered. The balloon was launched on 24 January 2010 and remained aloft for about 13 h at a height of 34 km in Arctic polar vortex air (de Lange et al., 2012; Wetzel et al., 2012).

TELIS was equipped with receivers operating at 480–650 GHz (de Lange et al., 2010) and at 1.8 THz. The ClO profile was determined from the transition at 501.27 GHz, the same as SMR. The level-2 processing of the TELIS ClO measurements was done using the Tikhonov regularization (Tikhonov, 1963) described in detail

**SMILES CIO  
comparison**

H. Sagawa et al.

[Title Page](#)[Abstract](#)[Introduction](#)[Conclusions](#)[References](#)[Tables](#)[Figures](#)[◀](#)[▶](#)[◀](#)[▶](#)[Back](#)[Close](#)[Full Screen / Esc](#)[Printer-friendly Version](#)[Interactive Discussion](#)

by de Lange et al. (2012). In that paper, the TELIS CIO and HCl products were compared with the coincident measurements of Aura MLS. The difference between the TELIS and MLS CIO (version 2.2) profiles in daytime equilibrium was  $\sim 0.2$  ppbv at the CIO peak altitude, and was within the expected systematic biases of both instruments (de Lange et al., 2012). With respect to MIPAS-B, its low-level data processing including instrument characterization is described by Friedl-Vallon et al. (2004). Retrieval calculations of MIPAS-B measurements were performed with a least squares fitting algorithm using analytical derivative spectra. The Tikhonov-Phillips regularization approach constraining with respect to the form of an a priori profile was adopted. The CIO retrieval was carried out in the P-branch region of the  $11.8 \mu\text{m}$  band with an altitude resolution of about 2–5 km. A further overview of the MIPAS-B data analysis is given by Wetzel et al. (2012) and references therein.

In this section we compare the SMILES NICT v2.1.5 CIO profiles with those from TELIS (version 3.0 of its level-2 product) and MIPAS-B. The TELIS profile used in this study includes a correction for the non-linear response function of the detector, which was absent in the previous TELIS–MLS comparison by de Lange et al. (2012). Figure 11 shows the close coincident measurement locations of SMILES, TELIS and MIPAS-B. The SMILES tangent points for a tangent height of 23 km are shown by the black square symbols, and those of TELIS by blue circles. The SMILES measurement of the observation identifier 761 (tangent point at  $30.5^\circ \text{E}$ ,  $64.8^\circ \text{N}$ ) shows good coincidence with TELIS observations 14 932 ( $32.4^\circ \text{E}$ ,  $67.3^\circ \text{N}$ ), 17 611 ( $33.6^\circ \text{E}$ ,  $66.7^\circ \text{N}$ ), and 21 537 ( $34.0^\circ \text{E}$ ,  $64.7^\circ \text{N}$ ); the latter being the closest in terms of geophysical distance ( $\sim 160$  km). In case of MIPAS-B measurements, the sequences from 08a to 09b are the best candidates for comparison as these are conducted under virtually identical observation geometries as the TELIS observations 14932 and 17611. We used the MIPAS-B CIO profile that was retrieved from the averaged spectra of measurement sequences 08a–09b, improving the signal-to-noise ratios in the measurement which led to a higher vertical resolution. In addition, the SMILES measurement 760 ( $23.2^\circ \text{E}$ ,  $64.0^\circ \text{N}$ ) shows good coincidence with the Aura MLS measurements shown by stars on the map, and

**SMILES CIO  
comparison**

H. Sagawa et al.

[Title Page](#)[Abstract](#)[Introduction](#)[Conclusions](#)[References](#)[Tables](#)[Figures](#)[◀](#)[▶](#)[◀](#)[▶](#)[Back](#)[Close](#)[Full Screen / Esc](#)[Printer-friendly Version](#)[Interactive Discussion](#)

therefore we also included them in this comparison. On the background of Fig. 11, the spatial distribution of the potential vorticity (PV) at the isentropic surface (potential temperature of 530 K which corresponds to approximately 19 km) is also shown in order to see the vortex activity at that day. The PV data were taken from the European Centre for Medium-Range Weather Forecasts (ECMWF) analysis for 12:00 UTC of 24 January 2010.

Figure 12 shows the CIO profiles derived from the SMILES, TELIS, MIPAS-B, and MLS measurements. As described in Sect. 3, we convolved the TELIS and MLS profiles with the SMILES averaging kernels (middle plot of Fig. 12). And for the comparison including MIPAS-B, both of the SMILES and MIPAS-B averaging kernel matrices were considered (right plot of Fig. 12). In general the SMILES NICT v2.1.5 CIO profiles detected the CIO enhancement in the lower stratosphere to a satisfactory extent despite its limited sensitivity at these altitudes. The SMILES CIO VMR profiles from the measurements 760 and 761 are almost identical and show the largest CIO enhancement compared to the others. From the SMILES-averaging kernel convolved comparison it follows that the SMILES peak values are +0.4 ppbv (16 %) and +0.2 ppbv (8 %) larger than respectively TELIS and MLS. The expected systematic error is  $\sim 10\%$  for both SMILES and TELIS at 23 km ( $\sim 25$  hPa) (de Lange et al., 2012). This corresponds to 0.25 ppbv (SMILES) and 0.2 ppbv (TELIS), giving a total uncertainty of 0.32 ppbv in rss. The observed difference between SMILES and TELIS is significantly larger than this systematic error. Below the CIO peak altitude the SMILES profiles become more similar to the MLS results, while at altitudes above the peak they show good agreement with those of TELIS. Looking to the comparison with MIPAS-B, the amplitude of CIO enhancement derived by TELIS is fairly consistent with that derived by the MIPAS-B measurements. It is most likely that the SMILES NICT profiles have a positive bias in the lower stratosphere, which is consistent with the comparison with the SMILES JAXA level-2 product (see Sect. 4.2.2). It should be noted that the SMILES (and MLS) measurements are rather on the edge of the vortex (as shown by the strong gradient of the PV surface) with horizontal resolutions of  $\sim 500$ – $1000$  km, and therefore even a small

mismatch in the geolocations, SZAs, or in the observation LOS directions between the coincident profiles could yield variabilities of the ClO distribution along each instrument's LOS. Therefore, we consider it difficult to quantitatively discuss bias errors of SMILES ClO only from this coincidence comparisons. This situation can be improved by future studies using outputs of chemical models for statistical comparison.

## 6 Conclusion

SMILES has provided a unique dataset of global (38° S–65° N) ClO observations from the lower stratosphere up to the mesosphere. Its high sensitivity has revealed the distribution of ClO in the mesosphere and the non sun-synchronous orbit allowed us to follow its diurnal variation. It is thus an important database for advancing our understanding of atmospheric chemistry.

We compared the SMILES ClO profiles processed at NICT with those generated by the JAXA level-2 chain, and with measurements of several satellite and balloon-borne instruments. The difference between the retrieval configurations of the NICT v2.1.5 and the JAXA operational code v2.1 processings resulted in a ClO difference of 15 pptv at 4 hPa for daytime and 10 pptv at 2 hPa for nighttime measurements. These differences are within the estimated systematic error of the NICT v2.1.5 processing. In the nighttime lower stratosphere where ClO VMRs are known to decrease to zero, the NICT v2.1.5 ClO profiles show negative VMRs of about –30 pptv. The cause for this bias is considered to be the use of the limited spectral bandwidth in the NICT processing which introduces contaminations from other broadened spectral signals. This seems to have also affected the NICT v2.1.5 ClO profiles from chlorine-activated polar vortex conditions, where the NICT v2.1.5 data showed 0.3 ppbv (30%) larger VMRs at 50 hPa compared to the JAXA v2.1 product. This issue should be solved in the next version of the NICT level processing, implementing a broader spectral bandwidth in the data analysis.

## SMILES ClO comparison

H. Sagawa et al.

Title Page

Abstract

Introduction

Conclusions

References

Tables

Figures

◀

▶

◀

▶

Back

Close

Full Screen / Esc

Printer-friendly Version

Interactive Discussion



**SMILES CIO  
comparison**

H. Sagawa et al.

Title Page

Abstract

Introduction

Conclusions

References

Tables

Figures

◀

▶

◀

▶

Back

Close

Full Screen / Esc

Printer-friendly Version

Interactive Discussion



The comparisons of SMILES NICT v2.1.5 CIO profile with those of Aura MLS (version 3.3) and Odin SMR (Chalmers level-2 version 2.1) were carried out for the low and middle latitude region in order to verify the SMILES data quality at different local times. The SMILES CIO daytime profiles agree well (differences within 0.04 ppbv) with those of MLS after correcting for the known negative bias of MLS. Comparison with the Odin SMR data pointed out that SMR CIO profiles have a negative bias in the mesosphere (0.1 hPa). The difference between SMILES and SMR CIO profiles were fairly consistent with the findings of previous MLS–SMR comparisons. The zonal average distribution for northern winter (January–March, 2010) was compared between SMILES and Envisat MIPAS (version V5R\_CIO\_220 of the IMK/IAA product). In general, both datasets were in good agreement, showing the latitudinal variation of CIO VMR at the lower stratosphere (smaller VMRs at the equator) and similar diurnal variation. In addition, we compared the SMILES CIO profiles inside the polar vortex with those measured by TELIS and MIPAS-B. Despite of its degraded sensitivity to the lower stratosphere, the NICT v2.1.5 product of the SMILES CIO profiles detected the CIO enhancement (~ 2.5 ppbv at 23 km) to a satisfactory extent. This observed enhancement was slightly larger than those of TELIS and MIPAS-B, although differences in the observation geometries and horizontal resolutions should be taken into account for further quantitative discussion.

In conclusion, we found that the NICT-processed SMILES CIO profiles generally agree well with other measurements. No significant bias as a function of local time was detected outside the polar region. This means that the SMILES dataset can be scientifically used as a reference for the diurnal variation of CIO. For the lower stratosphere in the nighttime (altitudes below 30 hPa level) and inside the chlorine-activated polar vortex, the current version of the SMILES NICT CIO product shows systematic biases, though not fatal, due to the configuration in the retrieval analysis. This will be improved in the next version of the NICT level-2 processing.

**SMILES CIO  
comparison**

H. Sagawa et al.

Title Page

Abstract

Introduction

Conclusions

References

Tables

Figures

◀

▶

◀

▶

Back

Close

Full Screen / Esc

Printer-friendly Version

Interactive Discussion



*Acknowledgements.* SMILES is a collaborative project of the National Institute of Information and Communications Technology (NICT) and the Japan Aerospace Exploration Agency (JAXA). The SMILES NICT level-2 data processing was supported by J. Möller (Molflow Co., Ltd.) and by K. Muranaga and T. Haru (SEC Co., Ltd.). The author HS is grateful to C. Mitsuda (Fujitsu F. I. P. Corp.) and the SMILES level-2 team in JAXA for their valuable discussions on the SMILES internal comparison. We thank K. Suzuki (Tokyo University), Y. Onodera and K. Kita (Ibaraki University) for their contribution to the comparison of early versions of the SMILES NICT products. Work at the Jet Propulsion Laboratory, California Institute of Technology was performed under contract with the National Aeronautics and Space Administration. Odin is a Swedish-led satellite project funded jointly by Sweden (SNSB), Canada (CSA), Finland (TEKES), France (CNES), and the Third Party Mission program of the European Space Agency (ESA). TELIS is a collaboration project of the Deutsche Zentrum für Luft- und Raumfahrt (DLR) in Germany, the Rutherford Appleton Laboratory (RAL) in the UK, and the Netherlands Institute for Space Research (SRON) in the Netherlands. We are grateful to the MIPAS balloon team at Karlsruhe Institute of Technology (KIT), the TELIS balloon team at DLR and SRON, and the Swedish Space Corporation (SSC) Esrange people for excellent balloon operations and data processing. The author TOS is supported by a Grant in Aid for Research Fellowship for Young Scientists DC1 (No. 23-9766) from the Japan Society for the Promotion of Science.

**References**

- Aellig, C. P., Kämpfer, N., Rudin, C., Bevilacqua, R. M., Degenhardt, W., Hartogh, P., Jarchow, C., Künzi, K., Olivero, J. J., Croskey, C., Waters, J. W., and Michelsen, H. A.: Latitudinal distribution of upper stratospheric CIO as derived from Space Borne Microwave Spectroscopy, *Geophys. Res. Lett.*, 23, 2321–2324, doi:10.1029/96GL01215, 1996. 630
- Baron, P., Ricaud, P., de La Noë, J., Eriksson, J. E. P., Merino, F., Ridal, M., and Murtagh, D. P.: Studies for the Odin sub-millimetre radiometer, II. Retrieval methodology, *Can. J. Phys.*, 80, 341–356, doi:10.1139/p01-150, 2002. 620
- Baron, P., Urban, J., Sagawa, H., Möller, J., Murtagh, D. P., Mendrok, J., Dupuy, E., Sato, T. O., Ochiai, S., Suzuki, K., Manabe, T., Nishibori, T., Kikuchi, K., Sato, R., Takayanagi, M., Murayama, Y., Shiotani, M., and Kasai, Y.: The Level 2 research product algorithms for the Su-

**SMILES ClO  
comparison**

H. Sagawa et al.

Title Page

Abstract

Introduction

Conclusions

References

Tables

Figures

◀

▶

◀

▶

Back

Close

Full Screen / Esc

Printer-friendly Version

Interactive Discussion



perconducting Submillimeter-Wave Limb-Emission Sounder (SMILES), *Atmos. Meas. Tech.*, 4, 2105–2124, doi:10.5194/amt-4-2105-2011, 2011. 619, 620, 626, 627

Barret, B., Ricaud, P., Santee, M. L., Attié, J.-L., Urban, J., Le Flochmoën, E., Berthet, G., Murtagh, D., Eriksson, P., Jones, A., de La Noë, J., Dupuy, E., Froidevaux, L., Livesey, N. J., Waters, J. W., and Filipiak, M. J.: Intercomparisons of trace gases profiles from the Odin/SMR and Aura/MLS limb sounders, *J. Geophys. Res.-Atmos.*, 111, D21302, doi:10.1029/2006JD007305, 2006. 633

Birk, M., Wagner, G., de Lange, G., de Lange, A., Ellison, B. N., Harman, M. R., Murk, A., Oelhaf, H., Maucher, G., and Sartorius, C.: TELIS: TERahertz and subMMW Limb sounder – project summary after first successful flight, in: *Twenty-First International Symposium on Space Terahertz Technology*, 195–200, 2010. 616

de Lange, A., Birk, M., de Lange, G., Friedl-Vallon, F., Kiselev, O., Koshelets, V., Maucher, G., Oelhaf, H., Selig, A., Vogt, P., Wagner, G., and Landgraf, J.: HCl and ClO in activated Arctic air; first retrieved vertical profiles from TELIS submillimetre limb spectra, *Atmos. Meas. Tech.*, 5, 487–500, doi:10.5194/amt-5-487-2012, 2012. 637, 638, 639

de Lange, G., Birk, M., Boersma, D., Dercksen, J., Dmitriev, P., Ermakov, A. B., Filippenko, L. V., Golstein, H., Hoogeveen, R. W. M., de Jong, L., Khudchenko, A. V., Kinev, N. V., Kiselev, O. S., van Kuik, B., de Lange, A., van Rantwijk, J., Selig, A. M., Sobolev, A. S., Torgashin, M. Y., de Vries, E., Wagner, G., Yagoubov, P. A., and Koshelets, V. P.: Development and characterization of the superconducting integrated receiver channel of the TELIS atmospheric sounder, *Supercond. Sci. Tech.*, 23, 045016, doi:10.1088/0953-2048/23/4/045016, 2010. 637

Dupuy, E., Walker, K. A., Kar, J., Boone, C. D., McElroy, C. T., Bernath, P. F., Drummond, J. R., Skelton, R., McLeod, S. D., Hughes, R. C., Nowlan, C. R., Dufour, D. G., Zou, J., Nichitiu, F., Strong, K., Baron, P., Bevilacqua, R. M., Blumenstock, T., Bodeker, G. E., Borsdorff, T., Bourassa, A. E., Bovensmann, H., Boyd, I. S., Bracher, A., Brogniez, C., Burrows, J. P., Catoire, V., Ceccherini, S., Chabrillat, S., Christensen, T., Coffey, M. T., Cortesi, U., Davies, J., De Clercq, C., Degenstein, D. A., De Mazière, M., Demoulin, P., Dodion, J., Firanski, B., Fischer, H., Forbes, G., Froidevaux, L., Fussen, D., Gerard, P., Godin-Beekmann, S., Goutail, F., Granville, J., Griffith, D., Haley, C. S., Hannigan, J. W., Höpfner, M., Jin, J. J., Jones, A., Jones, N. B., Jucks, K., Kagawa, A., Kasai, Y., Kerzenmacher, T. E., Kleinböhl, A., Klekociuk, A. R., Kramer, I., Küllmann, H., Kuttippurath, J., Kyrölä, E., Lambert, J.-C., Livesey, N. J., Llewellyn, E. J., Lloyd, N. D., Mahieu, E., Manney, G. L., Marshall, B. T., McConnell, J. C., Mc-

**SMILES ClO  
comparison**

H. Sagawa et al.

Title Page

Abstract

Introduction

Conclusions

References

Tables

Figures

◀

▶

◀

▶

Back

Close

Full Screen / Esc

Printer-friendly Version

Interactive Discussion



Cormick, M. P., McDermid, I. S., McHugh, M., McLinden, C. A., Mellqvist, J., Mizutani, K., Murayama, Y., Murtagh, D. P., Oelhaf, H., Parrish, A., Petelina, S. V., Piccolo, C., Pommereau, J.-P., Randall, C. E., Robert, C., Roth, C., Schneider, M., Senten, C., Steck, T., Strandberg, A., Strawbridge, K. B., Sussmann, R., Swart, D. P. J., Tarasick, D. W., Taylor, J. R., Tétard, C., Thomason, L. W., Thompson, A. M., Tully, M. B., Urban, J., Vanhellemont, F., Vigouroux, C., von Clarmann, T., von der Gathen, P., von Savigny, C., Waters, J. W., Witte, J. C., Wolff, M., and Zawodny, J. M.: Validation of ozone measurements from the Atmospheric Chemistry Experiment (ACE), *Atmos. Chem. Phys.*, 9, 287–343, doi:10.5194/acp-9-287-2009, 2009. 624

Fischer, H., Birk, M., Blom, C., Carli, B., Carlotti, M., von Clarmann, T., Delbouille, L., Dudhia, A., Ehnhalt, D., Endemann, M., Flaud, J. M., Gessner, R., Kleinert, A., Koopman, R., Langen, J., López-Puertas, M., Mosner, P., Nett, H., Oelhaf, H., Perron, G., Remedios, J., Ridolfi, M., Stiller, G., and Zander, R.: MIPAS: an instrument for atmospheric and climate research, *Atmos. Chem. Phys.*, 8, 2151–2188, doi:10.5194/acp-8-2151-2008, 2008. 616, 634

Friedl-Vallon, F., Maucher, G., Seefeldner, M., Trieschmann, O., Kleinert, A., Lengel, A., Keim, C., Oelhaf, H., and Fischer, H.: Design and characterization of the Balloon-Borne Michelson Interferometer for Passive Atmospheric Sounding (MIPAS-B2), *Appl. Optics*, 43, 3335–3355, doi:10.1364/AO.43.003335, 2004. 616, 638

Glatthor, N., von Clarmann, T., Fischer, H., Grabowski, U., Höpfner, M., Kellmann, S., Kiefer, M., Linden, A., Milz, M., Steck, T., Stiller, G. P., Mengistu Tsidu, G., Wang, D.-Y., and Funke, B.: Spaceborne ClO observations by the Michelson Interferometer for Passive Atmospheric Sounding (MIPAS) before and during the Antarctic major warming in September/October 2002, *J. Geophys. Res.-Atmos.*, 109, D11307, doi:10.1029/2003JD004440, 2004. 635, 637

Khosravi, M., Baron, P., Urban, J., Froidevaux, L., Jonsson, A. I., Kasai, Y., Kuribayashi, K., Mitsuda, C., Murtagh, D. P., Sagawa, H., Santee, M. L., Sato, T. O., Shiotani, M., Suzuki, M., von Clarmann, T., Walker, K. A., and Wang, S.: Diurnal variation of stratospheric HOCl, ClO and HO<sub>2</sub> at the equator: comparison of 1-D model calculations with measurements of satellite instruments, *Atmos. Chem. Phys. Discuss.*, 12, 21065–21104, doi:10.5194/acpd-12-21065-2012, 2012. 617

Kikuchi, K., Nishibori, T., Ochiai, S., Ozeki, H., Irimajiri, Y., Kasai, Y., Koike, M., Manabe, T., Mizukoshi, K., Murayama, Y., Nagahama, T., Sano, T., Sato, R., Seta, M., Takahashi, C., Takayanagi, M., Masuko, H., Inatani, J., Suzuki, M., and Shiotani, M.: Overview and early

**SMILES CIO  
comparison**

H. Sagawa et al.

Title Page

Abstract

Introduction

Conclusions

References

Tables

Figures

◀

▶

◀

▶

Back

Close

Full Screen / Esc

Printer-friendly Version

Interactive Discussion



- results of the Superconducting Submillimeter-Wave Limb-Emission Sounder (SMILES), *J. Geophys. Res.-Atmos.*, 115, D23306, doi:10.1029/2010JD014379, 2010. 616, 619
- Livesey, J. N., Read, W. G., Froidevaux, L., Lambert, A., Manney, G. L., Pumphrey, H. C., Santee, M. L., Schwartz, M. J., Wang, S., Cofield, R. E., Cuddy, D. T., Fuller, R. A., Jarnot, R. F., Jiang, J. H., Knosp, B. W., Stek, P. C., Wagner, P. A., and Wu, D. L.: Version 3.3 level 2 data quality and description document, Tech. Rep., JPL D-33509, Jet Propulsion Laboratory, available at: <http://mls.jpl.nasa.gov/data/datadocs.php> (last access: 18 December 2012), 2011. 625, 632, 633, 634
- Livesey, N. J., van Snyder, W., Read, W. G., and Wagner, P. A.: Retrieval algorithms for the EOS Microwave Limb Sounder (MLS), *IEEE T. Geosci. Remote*, 44, 1144–1155, doi:10.1109/TGRS.2006.872327, 2006. 631
- Manney, G. L., Daffer, W. H., Zawodny, J. M., Bernath, P. F., Hoppel, K. W., Walker, K. A., Knosp, B. W., Boone, C., Remsberg, E. E., Santee, M. L., Harvey, V. L., Pawson, S., Jackson, D. R., Deaver, L., McElroy, C. T., McLinden, C. A., Drummond, J. R., Pumphrey, H. C., Lambert, A., Schwartz, M. J., Froidevaux, L., McLeod, S., Takacs, L. L., Suarez, M. J., Trepte, C. R., Cuddy, D. C., Livesey, N. J., Harwood, R. S., and Waters, J. W.: Solar occultation satellite data and derived meteorological products: sampling issues and comparisons with Aura Microwave Limb Sounder, *J. Geophys. Res.-Atmos.*, 112, D24S50, doi:10.1029/2007JD008709, 2007. 630
- Merino, F., Murtagh, D. P., Ridal, M., Eriksson, P., Baron, P., Ricaud, P., and de La Noë, J.: Studies for the Odin sub-millimetre radiometer, III. Performance simulations, *Can. J. Phys.*, 80, 357–373, doi:10.1139/p01-154, 2002. 620
- Murtagh, D., Frisk, U., Merino, F., Ridal, M., Jonsson, A., Stegman, J., Witt, G., Eriksson, P., Jiménez, C., Megie, G., de La Noë, J., Ricaud, P., Baron, P., Pardo, J. R., Hauchcorne, A., Llewellyn, E. J., Degenstein, D. A., Gattinger, R. L., Lloyd, N. D., Evans, W. F. J., McDade, I. C., Haley, C. S., Sioris, C., von Savigny, C., Solheim, B. H., McConnell, J. C., Strong, K., Richardson, E. H., Leppelmeier, G. W., Kyrölä, E., Auvinen, H., and Oikarinen, L.: An overview of the Odin atmospheric mission, *Can. J. Phys.*, 80, 309–318, doi:10.1139/p01-157, 2002. 616, 633
- Ochiai, S., Kikuchi, K., Nishibori, T., Manabe, T., Ozeki, H., Mizukoshi, K., Ohtsubo, F., Tsubosaka, K., Irimajiri, Y., Sato, R., and Shiotani, M.: Performance of JEM/SMILES in orbit, in: *Twenty-First International Symposium on Space Terahertz Technology*, 179–184, 2010. 619

---

**SMILES ClO  
comparison**

H. Sagawa et al.

---

[Title Page](#)
[Abstract](#)[Introduction](#)[Conclusions](#)[References](#)[Tables](#)[Figures](#)[◀](#)[▶](#)[◀](#)[▶](#)[Back](#)[Close](#)[Full Screen / Esc](#)[Printer-friendly Version](#)[Interactive Discussion](#)

- Oh, J. and Cohen, E. A.: Pressure broadening of ClO by N<sub>2</sub> and O<sub>2</sub> near 204 and 649 GHz and new frequency measurements between 632 and 725 GHz, *J. Quant. Spectrosc. Ra.*, 52, 151–156, doi:10.1016/0022-4073(94)90004-3, 1994. 622, 627, 629, 649
- 5 Pickett, H. M., Poynter, R. L., Cohen, E. A., Delitsky, M. L., Pearson, J. C., and Müller, H. S. P.: Submillimeter, millimeter and microwave spectral line catalog, *J. Quant. Spectrosc. Ra.*, 60, 883–890, doi:10.1016/S0022-4073(98)00091-0, 1998. 622, 627, 649
- Reber, C. A., Trevathan, C. E., McNeal, R. J., and Luther, M. R.: The Upper Atmosphere Research Satellite (UARS) mission, *J. Geophys. Res.*, 98, 10643, doi:10.1029/92JD02828, 1993. 616
- 10 Rodgers, C. D.: Retrieval of Atmospheric Temperature and Composition From Remote Measurements of Thermal Radiation, *Rev. Geophys. Space Phys.*, 14, 609–624, 1976. 619
- Rodgers, C. D.: Characterization and error analysis of profiles retrieved from remote sounding measurements, *J. Geophys. Res.*, 95, 5587–5595, doi:10.1029/JD095iD05p05587, 1990. 619
- 15 Rodgers, C. D.: Inverse methods for atmospheric sounding: theory and practice, in: *Series on Atmospheric, Oceanic and Planetary Physics*, World Scientific, 2, 3605–3609, 2000. 619
- Rodgers, C. D. and Connor, B. J.: Intercomparison of remote sounding instruments, *J. Geophys. Res.-Atmos.*, 108, 4116, doi:10.1029/2002JD002299, 2003. 624
- Santee, M. L., Lambert, A., Read, W. G., Livesey, N. J., Manney, G. L., Cofield, R. E.,  
20 Cuddy, D. T., Daffer, W. H., Drouin, B. J., Froidevaux, L., Fuller, R. A., Jarnot, R. F., Knosp, B. W., Perun, V. S., Snyder, W. V., Stek, P. C., Thurstans, R. P., Wagner, P. A., Waters, J. W., Connor, B., Urban, J., Murtagh, D., Ricaud, P., Barret, B., Kleinböhl, A., Kuttipurath, J., Küllmann, H., von Hobe, M., Toon, G. C., and Stachnik, R. A.: Validation of the Aura Microwave Limb Sounder ClO measurements, *J. Geophys. Res.-Atmos.*, 113, D15S22, doi:10.1029/2007JD008762, 2008. 632, 633, 634
- 25 Sato, T. O., Sagawa, H., Kreyling, D., Manabe, T., Ochiai, S., Kikuchi, K., Baron, P., Mendrok, J., Urban, J., Murtagh, D., Yasui, M., and Kasai, Y.: Strato-mesospheric ClO observations by SMILES: error analysis and diurnal variation, *Atmos. Meas. Tech.*, 5, 2809–2825, doi:10.5194/amt-5-2809-2012, 2012. 616, 617, 620, 621, 622, 623
- 30 Solomon, S. and Garcia, R. R.: On the distributions of long-lived tracers and chlorine species in the middle atmosphere, *J. Geophys. Res.*, 89, 11633–11644, doi:10.1029/JD089iD07p11633, 1984. 630

**SMILES ClO  
comparison**

H. Sagawa et al.

Title Page

Abstract

Introduction

Conclusions

References

Tables

Figures

◀

▶

◀

▶

Back

Close

Full Screen / Esc

Printer-friendly Version

Interactive Discussion



- Suzuki, M., Mitsuda, C., Kikuchi, K., Nishibori, T., Ochiai, S., Ozeki, H., Sano, T., Mizobuchi, S., Takahashi, C., Manago, N., Imai, K., Naito, Y., Hayashi, H., Nishimoto, E., and Shiotani, M.: Overview of the Superconducting Submillimeter-Wave Limb-Emission Sounder (SMILES) and sensitivity to chlorine monoxide, ClO, IEEJ Transactions on Fundamentals and Materials, 132, 609–615, doi:10.1541/ieejfms.132.609, 2012. 619, 626
- Tikhonov, A.: On the solution of incorrectly stated problems and a method of regularization, Dokl. Akad. Nauk SSSR, 151, 501–504, 1963. 637
- Urban, J., Murtagh, D., Lautié, N., Barret, B., Dupuy, E., de LaNoë, J., Eriksson, P., Frisk, U., Jones, A., Le Flochmoën, E., Olberg, M., Piccolo, C., Ricauld, P., and Rösevall, J.: Odin/SMR Limb observations of trace gases in the polar lower stratosphere during 2004–2005, in: Atmospheric Science Conference, Vol. 628 of ESA Special Publication, 8–12 May 2006, Frascati, Italy, 1–6, 2006. 625, 633
- von Clarmann, T., Glatthor, N., Höpfner, M., Kellmann, S., Ruhnke, R., Stiller, G. P., Fischer, H., Funke, B., Gil-López, S., and López-Puertas, M.: Experimental evidence of perturbed odd hydrogen and chlorine chemistry after the October 2003 solar proton events, J. Geophys. Res.-Space, 110, A09S45, doi:10.1029/2005JA011053, 2005. 635
- von Clarmann, T., Höpfner, M., Kellmann, S., Linden, A., Chauhan, S., Funke, B., Grabowski, U., Glatthor, N., Kiefer, M., Schieferdecker, T., Stiller, G. P., and Versick, S.: Retrieval of temperature, H<sub>2</sub>O, O<sub>3</sub>, HNO<sub>3</sub>, CH<sub>4</sub>, N<sub>2</sub>O, ClONO<sub>2</sub> and ClO from MIPAS reduced resolution nominal mode limb emission measurements, Atmos. Meas. Tech., 2, 159–175, doi:10.5194/amt-2-159-2009, 2009. 635
- Waters, J. W., Froidevaux, L., Read, W. G., Manney, G. L., Elson, L. S., Flower, D. A., Jarnot, R. F., and Harwood, R. S.: Stratospheric ClO and ozone from the Microwave Limb Sounder on the Upper Atmosphere Research Satellite, Nature, 362, 597–602, doi:10.1038/362597a0, 1993. 616
- Waters, J. W., Froidevaux, L., Harwood, R. S., Jarnot, R. F., Pickett, H. M., Read, W. G., Siegel, P. H., Cofield, R. E., Filipiak, M. J., Flower, D. A., Holden, J. R., Lau, G. K., Livesey, N. J., Manney, G. L., Pumphrey, H. C., Santee, M. L., Wu, D. L., Cuddy, D. T., Lay, R. R., Loo, M. S., Perun, V. S., Schwartz, M. J., Stek, P. C., Thurstans, R. P., Boyles, M. A., Chandra, K. M., Chavez, M. C., Chen, G.-S., Chudasama, B. V., Dodge, R., Fuller, R. A., Girard, M. A., Jiang, J. H., Jiang, Y., Knosp, B. W., Labelle, R. C., Lam, J. C., Lee, A. K., Miller, D., Oswald, J. E., Patel, N. C., Pukala, D. M., Quintero, O., Scaff, D. M., Vansnyder, W., Tope, M. C., Wagner, P. A., and Walch, M. J.: The Earth Observing System

Microwave Limb Sounder (EOS MLS) on the Aura satellite, IEEE T. Geosci. Remote, 44, 1075–1092, doi:10.1109/TGRS.2006.873771, 2006. 616, 631

Wetzel, G., Oelhaf, H., Kirner, O., Friedl-Vallon, F., Ruhnke, R., Ebersoldt, A., Kleinert, A., Maucher, G., Nordmeyer, H., and Orphal, J.: Diurnal variations of reactive chlorine and nitrogen oxides observed by MIPAS-B inside the January 2010 Arctic vortex, Atmos. Chem. Phys., 12, 6581–6592, doi:10.5194/acp-12-6581-2012, 2012. 637, 638, 662

# AMTD

6, 613–663, 2013

## SMILES CIO comparison

H. Sagawa et al.

Title Page

Abstract

Introduction

Conclusions

References

Tables

Figures

⏪

⏩

◀

▶

Back

Close

Full Screen / Esc

Printer-friendly Version

Interactive Discussion



SMILES CIO  
comparison

H. Sagawa et al.

**Table 1.** Systematic error sources considered in this study. See the text for detailed explanation about the inversion model error.

Error source	Assumed uncertainty
Spectroscopic parameters of CIO	
Line position	Pickett et al. (1998) or Oh and Cohen (1994)
Line intensity	1%
Air pressure broadening, $\gamma$	3%
Temperature dependence of $\gamma$	10%
Other absorption coefficient parameters in the radiative transfer model	
Dry air continuum	20%
Instrumental function	
Non linearity correction of the gain	20% on the gain compression factor
AOS response function	10% of the FWHM
Image band contamination	footnote <sup>a</sup>
Antenna scanning pattern	footnote <sup>b</sup>
Inversion model	
Null space error due to use of fixed a priori values	

<sup>a</sup> Comparison between an ideal rejection rate for the image sideband signal and the realistic one.

<sup>b</sup> Comparison between the cases with and without considering the vertical movement of the antenna FOV during a single spectrum integration.

Title Page

Abstract

Introduction

Conclusions

References

Tables

Figures

◀

▶

◀

▶

Back

Close

Full Screen / Esc

Printer-friendly Version

Interactive Discussion



SMILES ClO  
comparison

H. Sagawa et al.

**Table 2.** Summary of the systematic error and precision at selected pressure levels for SMILES NICT v2.1.5 ClO profiles. The relative systematic errors are shown in the parenthesis. Precisions are 1- $\sigma$  standard deviation of the random error for a single-scan measurement. For the chlorine-activated polar vortex condition, only the errors for the lower stratosphere are shown.

Pressure	daytime mid-latitude		nighttime mid-latitude		chlorine-activated polar region	
	Systematic [pptv]	Precision [pptv]	Systematic [pptv]	Precision [pptv]	Systematic [pptv]	Precision [pptv]
$\leq 0.5$ hPa	5–10 (6–20 %)	30–150	3–15 (5–30 %)	30–150	–	–
4–2 hPa	30–35 (10 %)	30–40	4–9 (5 %)	30–40	–	–
80–20 hPa	5–10 ( $\geq 10$ %)	20–80	30 <sup>a</sup> (-%)	20–80	80–320 <sup>b</sup> (10–35 %)	30–160

<sup>a</sup> Based on the actual negative VMRs in the retrieved profiles.

<sup>b</sup> Errors for the pressure level of 30–80 hPa where the strong ClO enhancement occurs.

Title Page

Abstract

Introduction

Conclusions

References

Tables

Figures

◀

▶

◀

▶

Back

Close

Full Screen / Esc

Printer-friendly Version

Interactive Discussion



SMILES CIO  
comparison

H. Sagawa et al.

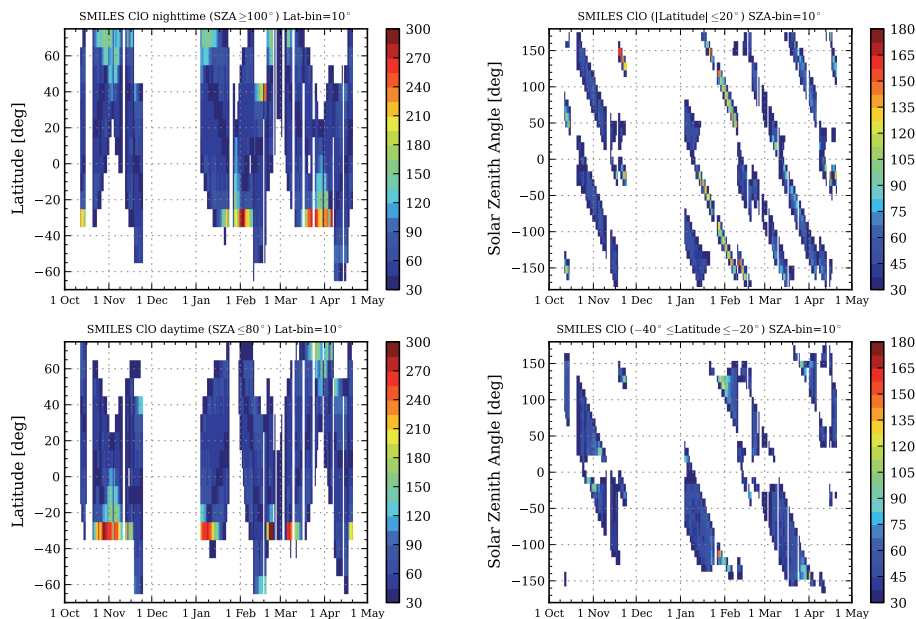


**Fig. 1.** Number of SMILES CIO measurements per day for the observation period (from 12 October 2009 to 21 April 2010). Left: measurement numbers summed over each latitudinal bin of  $10^\circ$  for each day. Upper and lower panels represent conditions for nighttime ( $SA \geq 100^\circ$ ) and daytime ( $SA \leq 80^\circ$ ), respectively. Right: measurement number as a function of observation date and SA. Upper and lower panels show data for latitudinal regions of  $20^\circ\text{S}$ – $20^\circ\text{N}$  and  $40^\circ\text{S}$ – $20^\circ\text{S}$ , respectively. Note that the negative sign for SA is simply an expedient representation used here which denotes the time range before noon.

Title Page

Abstract

Introduction

Conclusions

References

Tables

Figures

◀

▶

◀

▶

Back

Close

Full Screen / Esc

Printer-friendly Version

Interactive Discussion



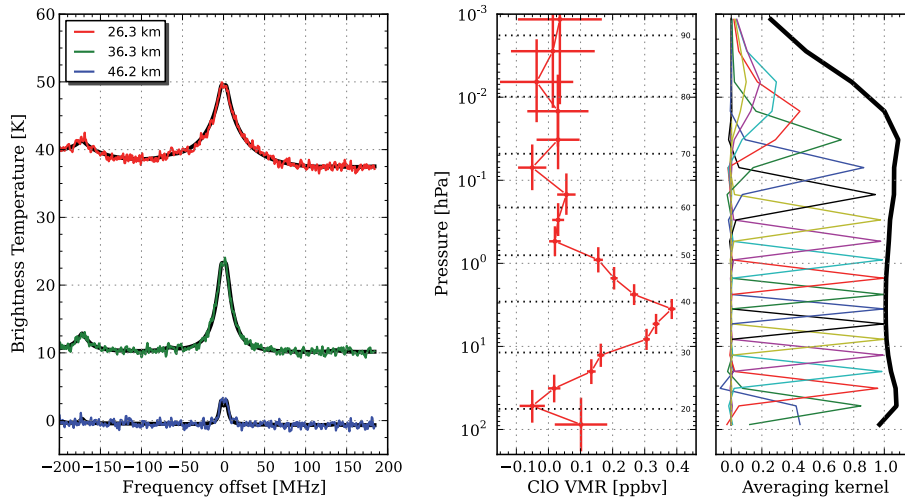


**Fig. 2.** Example SMILES CIO spectra, retrieved volume mixing ratio profile, and averaging kernels. Left: spectra from a single-scan observation obtained at ( $36^{\circ}$  E,  $18.9^{\circ}$  S), local time of 14:13 p.m. on 4 January 2010. Spectra from only three-tangent heights are shown as examples. Background black lines represent best-fit synthesis spectra after inversion analysis. The frequency axis is shown as an offset from the mean frequency (649.448 GHz) of CIO doublet lines. The spectral feature observed at  $-180$  MHz is an ozone isotope. Right: a sample CIO profile derived from a single-scan measurement, some of which are shown in the left panel, and the corresponding averaging kernels. Horizontal bars on CIO profile represent the  $1\text{-}\sigma$  of the retrieval error, vertical bars indicate the vertical resolution of the retrieval which is estimated from the width of the averaging kernels. Small numbers along the right edge represent corresponding altitude levels in km. Rightmost plot shows averaging kernels and measurement response, i.e. envelope of each averaging kernel. Each thin colored line shows the averaging kernels for the retrieved state at different altitudes. The thick black line represents the measurement response of the retrieval.

**SMILES CIO comparison**

H. Sagawa et al.

Title Page

Abstract Introduction

Conclusions References

Tables Figures

◀ ▶

◀ ▶

Back Close

Full Screen / Esc

Printer-friendly Version

Interactive Discussion



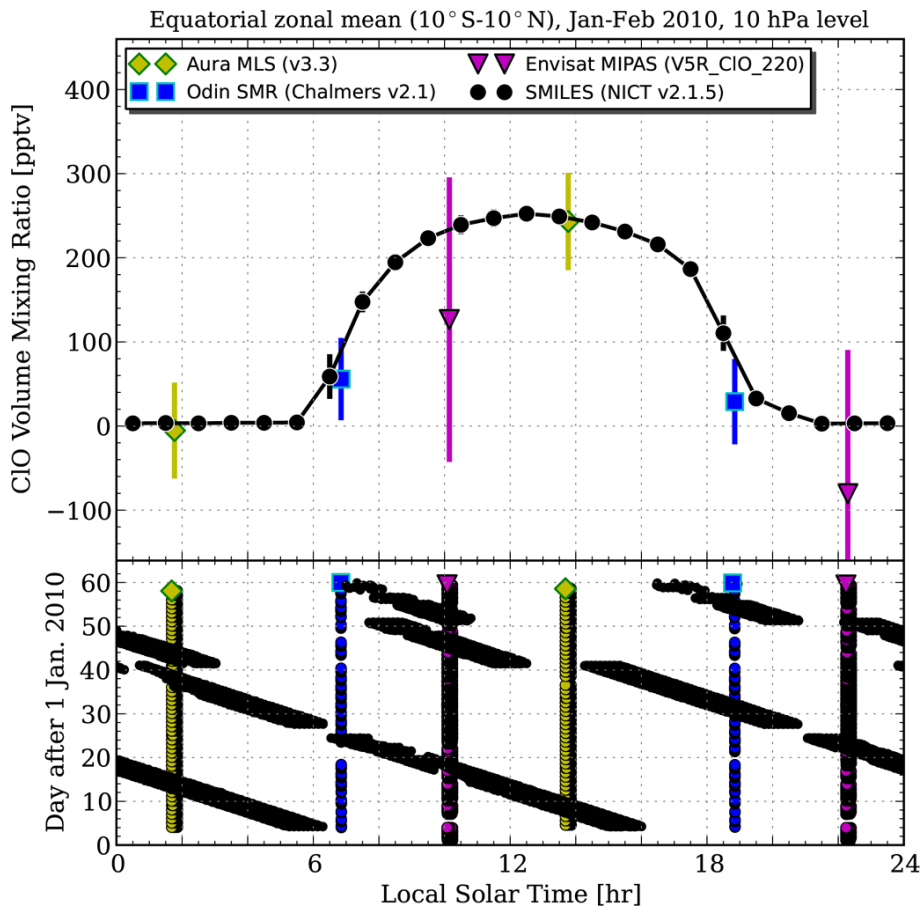


**Fig. 3.** Diurnal variation of CIO at 10 hPa observed by SMILES. Upper panel shows diurnal evolution of CIO VMR compared with measurements of Aura MLS, Odin SMR, and Envisat MIPAS. Vertical bars indicate the standard deviation ( $1\text{-}\sigma$ ) of the retrieved VMRs. Lower panel shows the sampling density of measurements in the local time plane.

SMILES ClO  
comparison

H. Sagawa et al.

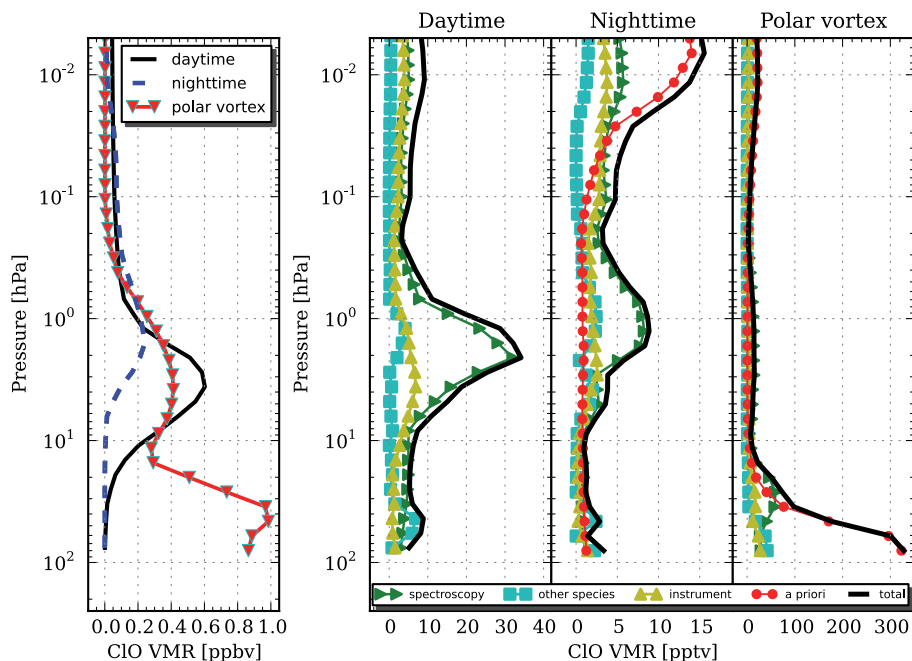


**Fig. 4.** Simulated systematic errors of SMILES ClO product (NICT v2.1.5). Left: reference ClO profiles used for synthesizing simulated spectra. Typical daytime, nighttime, and chlorine-enhanced polar air conditions were assumed. Right: estimated systematic errors for the considered ClO scenarios. See text for a description of the error sources.

Title Page

Abstract

Introduction

Conclusions

References

Tables

Figures

◀

▶

◀

▶

Back

Close

Full Screen / Esc

Printer-friendly Version

Interactive Discussion



SMILES ClO  
comparison

H. Sagawa et al.

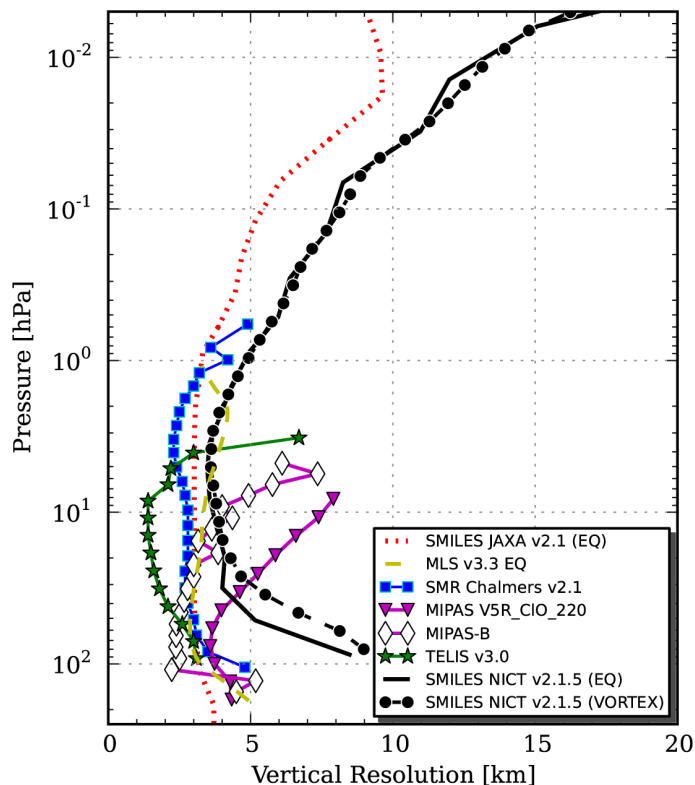


**Fig. 5.** Vertical resolutions of ClO measurements from the datasets considered in this study. Those for SMILES NICT v2.1.5 are shown in black lines for the equatorial region (solid line) and the chlorine-activated polar vortex condition (dotted-dashed line). The label “SMILES JAXA” represents the SMILES ClO product from the JAXA level-2 chain. The vertical resolution of MIPAS-B is that for the retrieval using averaged measurements (see Sect. 5.4).

Title Page

Abstract

Introduction

Conclusions

References

Tables

Figures

◀

▶

◀

▶

Back

Close

Full Screen / Esc

Printer-friendly Version

Interactive Discussion



SMILES CIO  
comparison

H. Sagawa et al.

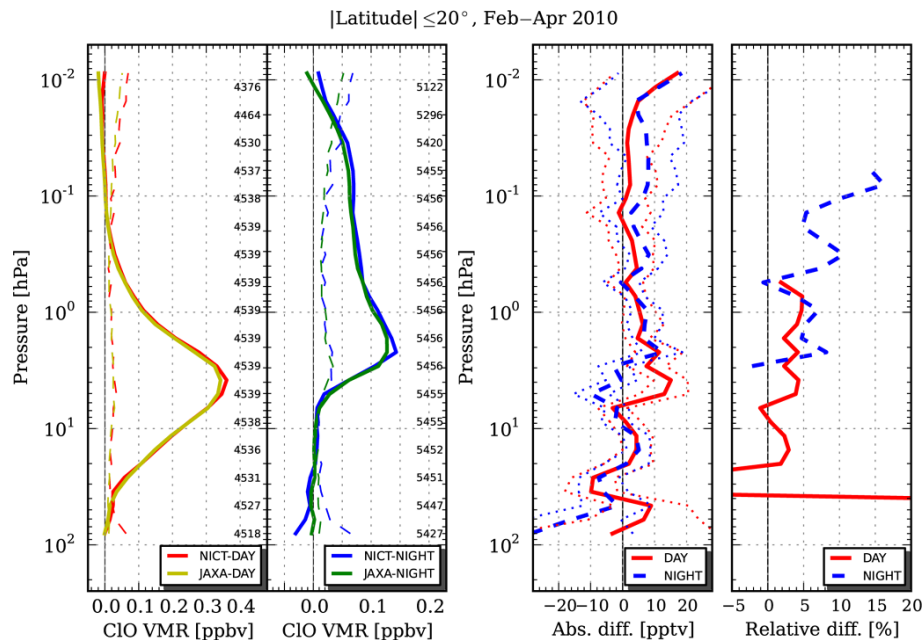


**Fig. 6.** Comparison of NICT v2.1.5 and JAXA v2.1 CIO profiles. Median VMR profiles are shown in the left panels. Daytime and nighttime data were separately averaged. Dashed lines show the 1-MAD of each dataset. Small numbers along the right vertical axes represent numbers of coincidence at that altitude level. Right two panels show absolute (left side) and relative (right side) differences between the two datasets.

Title Page

Abstract

Introduction

Conclusions

References

Tables

Figures

◀

▶

◀

▶

Back

Close

Full Screen / Esc

Printer-friendly Version

Interactive Discussion



SMILES ClO  
comparison

H. Sagawa et al.

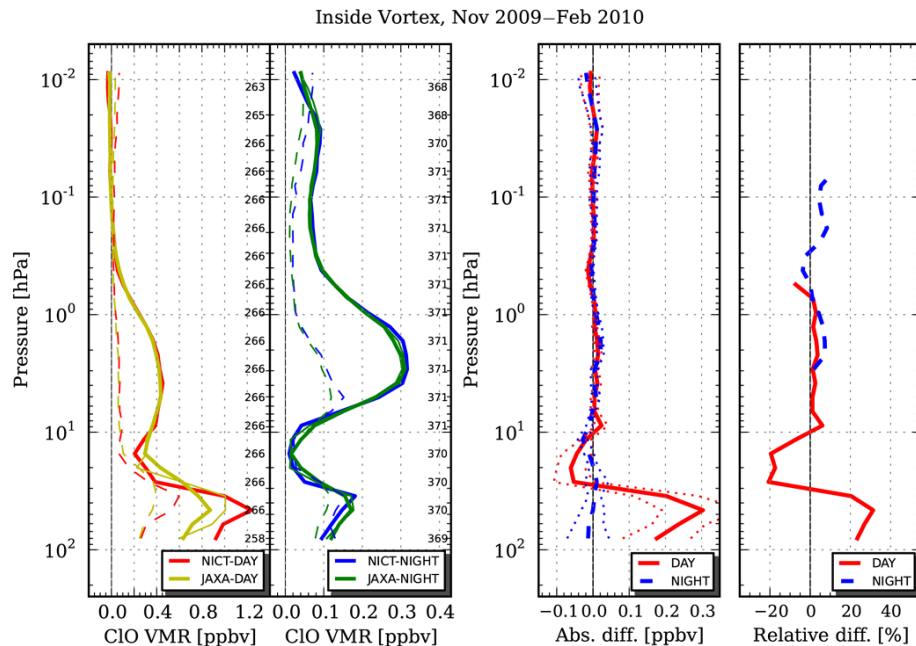


**Fig. 7.** Same as Fig. 6 except for polar vortex conditions. The thin and bold lines for the SMILES JAXA level-2 profiles represent before and after the convolution of the NICT v2.1.5 processing averaging kernels, i.e. thin line is the median of the raw JAXA level-2 profiles and bold is that of smoothed profiles. The absolute and relative differences are shown only for the smoothed case.

SMILES ClO  
comparison

H. Sagawa et al.

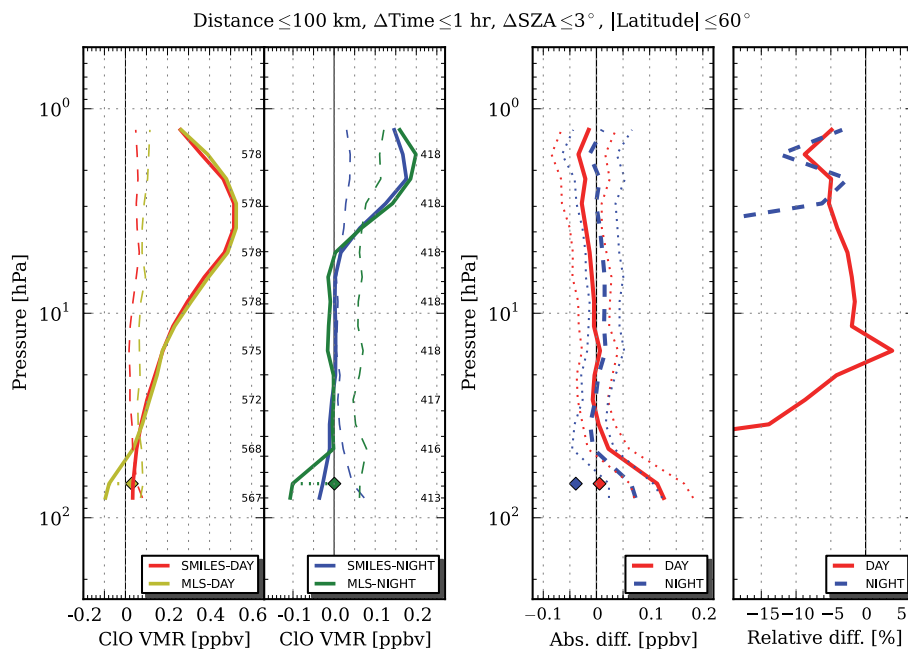


**Fig. 8.** Comparison of SMILES NICT ClO data with that of Aura MLS v3.3. Plot format is similar to that of Fig. 6. Diamond symbols on the ClO VMR profile plots represent MLS ClO VMRs after correcting for known bias for 68 hPa level (see text). The absolute differences between SMILES and the bias corrected MLS data at 68 hPa are also shown in diamond symbols.

Title Page

Abstract

Introduction

Conclusions

References

Tables

Figures

◀

▶

◀

▶

Back

Close

Full Screen / Esc

Printer-friendly Version

Interactive Discussion



SMILES ClO  
comparison

H. Sagawa et al.

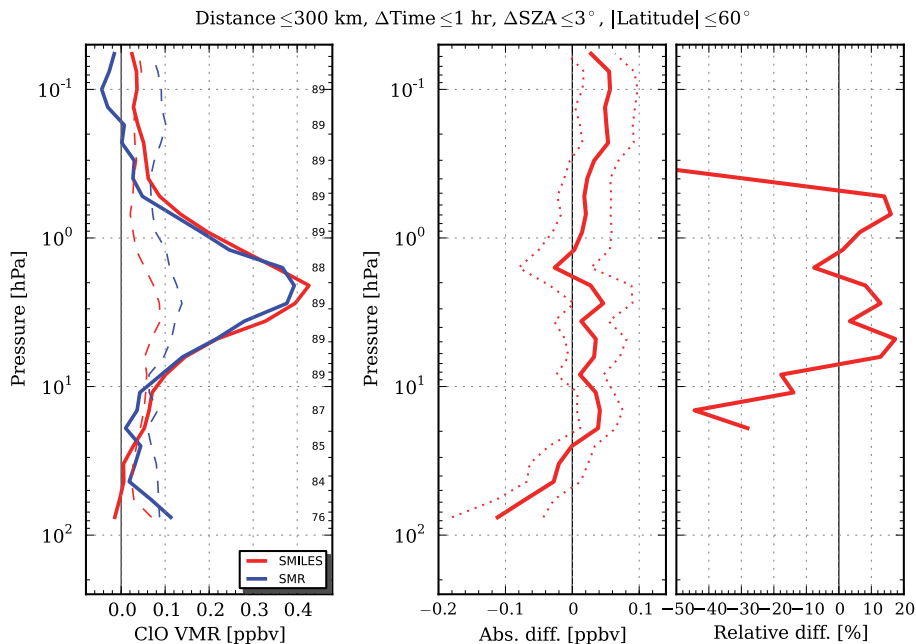


**Fig. 9.** Comparison of SMILES NICT ClO data with that of Odin SMR Chalmers-v2.1 product. Plot format is as similar as that of Fig. 6, except for not dividing the coincidences into daytime and nighttime cases.

Title Page

Abstract

Introduction

Conclusions

References

Tables

Figures

◀

▶

◀

▶

Back

Close

Full Screen / Esc

Printer-friendly Version

Interactive Discussion



SMILES CIO  
comparison

H. Sagawa et al.

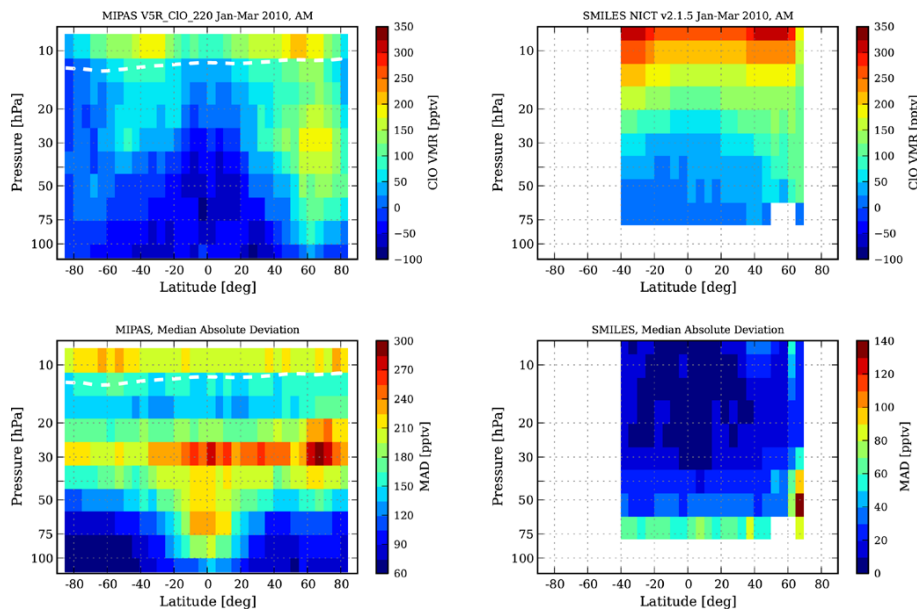


**Fig. 10.** Zonal median distributions of CIO data from MIPAS (left) and SMILES (right) measurements for daytime. See text for details of data selection. Bottom panels show median absolute deviations of zonal median plots. White dashed line indicates the approximate altitude level of 30 km, above which MIPAS data is not recommended for scientific use.

Title Page

Abstract

Introduction

Conclusions

References

Tables

Figures

◀

▶

◀

▶

Back

Close

Full Screen / Esc

Printer-friendly Version

Interactive Discussion



SMILES CIO  
comparison

H. Sagawa et al.

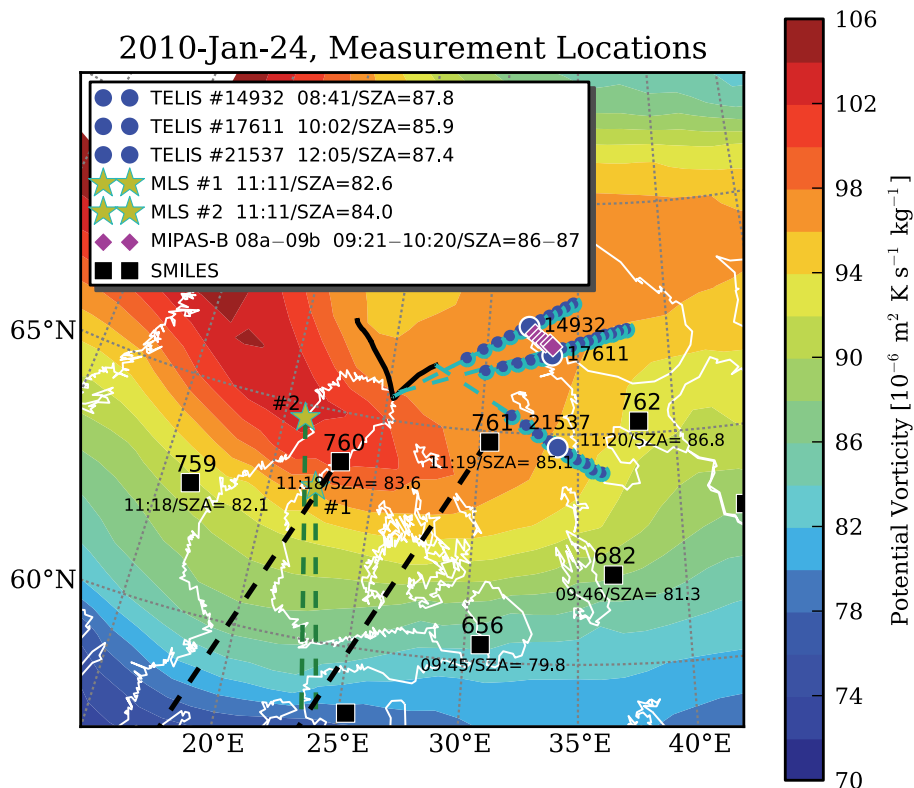


Fig. 11. Caption on next page.

Title Page

Abstract

Introduction

Conclusions

References

Tables

Figures

◀

▶

◀

▶

Back

Close

Full Screen / Esc

Printer-friendly Version

Interactive Discussion



## SMILES CIO comparison

H. Sagawa et al.

**Fig. 11.** Locations of selected SMILES, TELIS, MIPAS-B, and MLS measurements on 24 January 2010, superimposed on the potential vorticity distribution. Black squares represent SMILES measurement locations referring to the tangent point when SMILES pointed to a tangent height of 23 km. Observational lines-of-sight (LOS) are shown for some SMILES measurements as black dashed lines. The small number above each symbol is SMILES observation identification number. Corresponding local times and SZAs are indicated below the symbol. Blue circles represent the tangent points of TELIS measurements, for which the vertical scan started at  $\sim 9$  km. The black solid line represents the trajectory of the TELIS balloon gondola, and the blue dashed lines are the direction of the LOS towards each tangent point. The larger blue circles indicate the tangent points when TELIS looked at a tangent height of 23 km. Five-digit numbers on TELIS measurement locations indicate the observation identifier, with local time and SZA shown in legend. Stars represent two Aura MLS measurement locations with green dashed lines showing their LOSs. The measurement numbers for MLS are arbitrary ones prepared only for this study. The tangent points for the measurement sequences 08a–09b of MIPAS-B are shown in diamond symbols. The observation times and solar zenith angles changed from 09:21 to 10:20 and from  $87^\circ$  to  $86^\circ$  within those sequences (details can be found in the Figs. 1 and 2 given by Wetzell et al., 2012). The observation LOS is the same as that of TELIS 17611 measurement. The background color contour represents the potential vorticity (PV) field at the isentropic surface of 530 K (approximately 19 km), taken from the ECMWF analysis at 12:00 UTC on the same day as the observations.

Title Page

Abstract

Introduction

Conclusions

References

Tables

Figures

◀

▶

◀

▶

Back

Close

Full Screen / Esc

Printer-friendly Version

Interactive Discussion



SMILES ClO  
comparison

H. Sagawa et al.

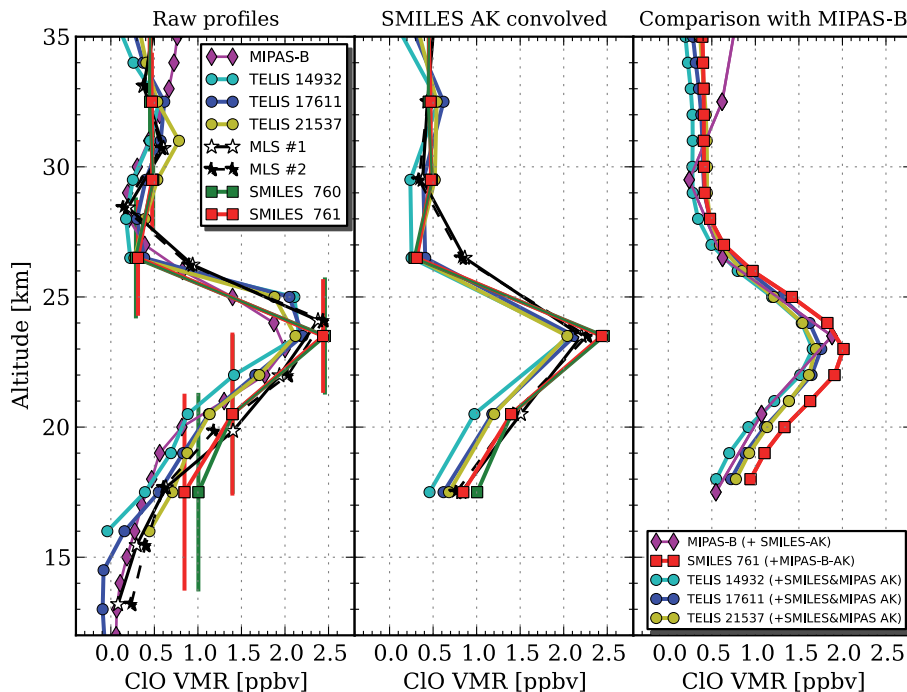


**Fig. 12.** ClO profiles derived from the SMILES v2.1.5, TELIS v3.0, MIPAS-B, and MLS v3-3 data. Left: original level-2 profiles without any smoothing. The vertical bars on the SMILES data indicate the vertical resolutions. Middle: TELIS and MLS profiles are convolved with the SMILES averaging kernels. Right: comparison with the MIPAS-B ClO profile. The SMILES profile from measurement 761 is convolved with the MIPAS-B averaging kernel matrix, and the MIPAS profile is convolved with the SMILES averaging kernels. For the TELIS measurements both of the SMILES and MIPAS-B averaging kernel matrices are considered.

Title Page

Abstract

Introduction

Conclusions

References

Tables

Figures

◀

▶

◀

▶

Back

Close

Full Screen / Esc

Printer-friendly Version

Interactive Discussion

